Maastricht University

Screening as a strategy to drive regenerative medicine research

Citation for published version (APA):

Vermeulen, S., & de Boer, J. (2021). Screening as a strategy to drive regenerative medicine research. *Methods*, *190*, 80-95. https://doi.org/10.1016/j.ymeth.2020.04.004

Document status and date:
Published: 01/06/2021

DOI:
10.1016/j.ymeth.2020.04.004

Document Version:
Accepted author manuscript (Peer reviewed / editorial board version)

Document license:
CC BY-NC-ND

Please check the document version of this publication:

• A submitted manuscript is the version of the article upon submission and before peer-review. There can be important differences between the submitted version and the official published version of record. People interested in the research are advised to contact the author for the final version of the publication, or visit the DOI to the publisher's website.
• The final author version and the galley proof are versions of the publication after peer review.
• The final published version features the final layout of the paper including the volume, issue and page numbers.

Link to publication

General rights
Copyright and moral rights for the publications made accessible in the public portal are retained by the authors and/or other copyright owners and it is a condition of accessing publications that users recognise and abide by the legal requirements associated with these rights.

• Users may download and print one copy of any publication from the public portal for the purpose of private study or research.
• You may not further distribute the material or use it for any profit-making activity or commercial gain
• You may freely distribute the URL identifying the publication in the public portal.

If the publication is distributed under the terms of Article 25fa of the Dutch Copyright Act, indicated by the “Taverne” license above, please follow below link for the End User Agreement:

www.umlib.nl/taverne-license

Take down policy
If you believe that this document breaches copyright please contact us at:

repository@maastrichtuniversity.nl

providing details and we will investigate your claim.

Download date: 05 May. 2024

Screening as a strategy to drive regenerative medicine research

Steven Vermeulen[1,2] and Jan de Boer[2]

[1]Laboratory for Cell Biology-Inspired Tissue Engineering, MERLN Institute, University of Maastricht, Maastricht, The Netherlands.

[2]BioInterface Science Group, Department of Biomedical Engineering and Institute for Complex Molecular Systems, University of Eindhoven, Eindhoven, The Netherlands

Abstract

In the field of regenerative medicine, optimization of the parameters leading to a desirable outcome remains a huge challenge. Examples include protocols for the guided differentiation of pluripotent cells towards specialized and functional cell types, phenotypic maintenance of primary cells in cell culture, or engineering of materials for improved tissue interaction with medical implants. This challenge originates from the enormous design space for biomaterials, chemical and biochemical compounds, and incomplete knowledge of the guiding biological principles. To tackle this challenge, high-throughput platforms allow screening of multiple perturbations in one experimental setup. In this review, we provide an overview of screening platforms that are used in regenerative medicine. We discuss their fabrication techniques, and *in silico* tools to analyze the extensive data sets typically generated by these platforms.

Introduction

A challenge in regenerative medicine is to control the complexity of biological systems. Advances have been made to control cell behavior leading to clinical applications *e.g.*, the differentiation of pluripotent cells towards primary cells [1] or the use of bioactive graft materials [2]. Many opportunities and challenges remain, such as the high incidence of catheter implant infections [3], the foreign body response against biomaterials [4], and the standing challenge to engineer functional tissues and organs *ex vivo*. Progress in these and other fields of regenerative medicine can be expedited if we can overcome current limitations in material design and increase our knowledge of biomaterial-cell interactions. Materials need to meet some requirements, for example, durability is a crucial factor in determining the success of the implant when supporting or replacing tissues [5]. At the same time, materials should not be cytotoxic or cause long-term harm in the body, as is often seen with breast implant ruptures or pathological encapsulation [6]. Furthermore, cell-biomaterial interaction should favor matrix deposition that allows optimal implant integration. Both physical and chemical properties can affect cell behavior. For example, a promising approach for bone tissue regeneration is the use of calcium phosphate particles, of which both chemistry (calcium phosphate) and structural properties (surface roughness) activate transcriptional profiles associated with bone induction [7]. This also reflects a challenge in finding the most optimal material design due to a large number of design parameters. For example, hundreds of different chemical compositions exist of the biocompatible and clinically applied material polyurethane [8].

To address the issues associated with incomplete information on both the biological and material side of the interface, methodologies that vary a large number of perturbations in one experimental setup can rapidly increase knowledge. Below, we highlight the potential of screening approaches where biology, material engineering, and computational science converge.

Biomaterials for High-Throughput Applications

During development and in the adult body, cells receive a wide variety of signals from their external environment. Therefore, much research focusses on appropriately controlling cell signaling *in vitro* for guiding cell behavior. This is not trivial because cells in standard culture conditions are exposed to different stimuli compared to physiological conditions. For example, standard culture media contains animal-derived serum, thus exposing cells to a-physiological cytokines and growth factors. In addition, flat tissue culture polystyrene has unique chemical and physical properties, which influence cell behavior. Therefore, it is not surprising that transferring cells from their native environment into cell culture often leads to substantial loss of *in situ* phenotypical identity. For example, chondrocytes that maintain cartilage homeostasis, quickly lose morphological characteristics and chondrogenic gene expression when cultured on tissue culture plastic [9]. Although an undesirable result, this does indicate

that the chemical and physical properties of the substrate on which cells grow has a profound effect on cell physiology and shows that we can use these properties to tweak cell behavior. In this section, we discuss different cell-biomaterial interfaces in a high-throughput setting in which large numbers of possibilities in chemical, biochemical, and structural biomaterial designs are used to control cells.

Surface Structures

Standard cell culture is carried out on flat surfaces. For cells, this is fundamentally different from their native 3D tissue environment. Therefore, physical cues in the form of surface structures are a promising tool for controlling cell behavior. However, a challenge is identifying the most optimal surface design that elicits a particular response. Surface structures can be constructed in variable height profiles, in a disordered or ordered manner, with different geometries, or by combining multiple profiles, thus creating hierarchical structures. Screening approaches can provide essential insight into this highly complex design space. In **Figure 1**, we provide the reader with a visualization of some high-throughput platforms, which we will be discussing in this section.

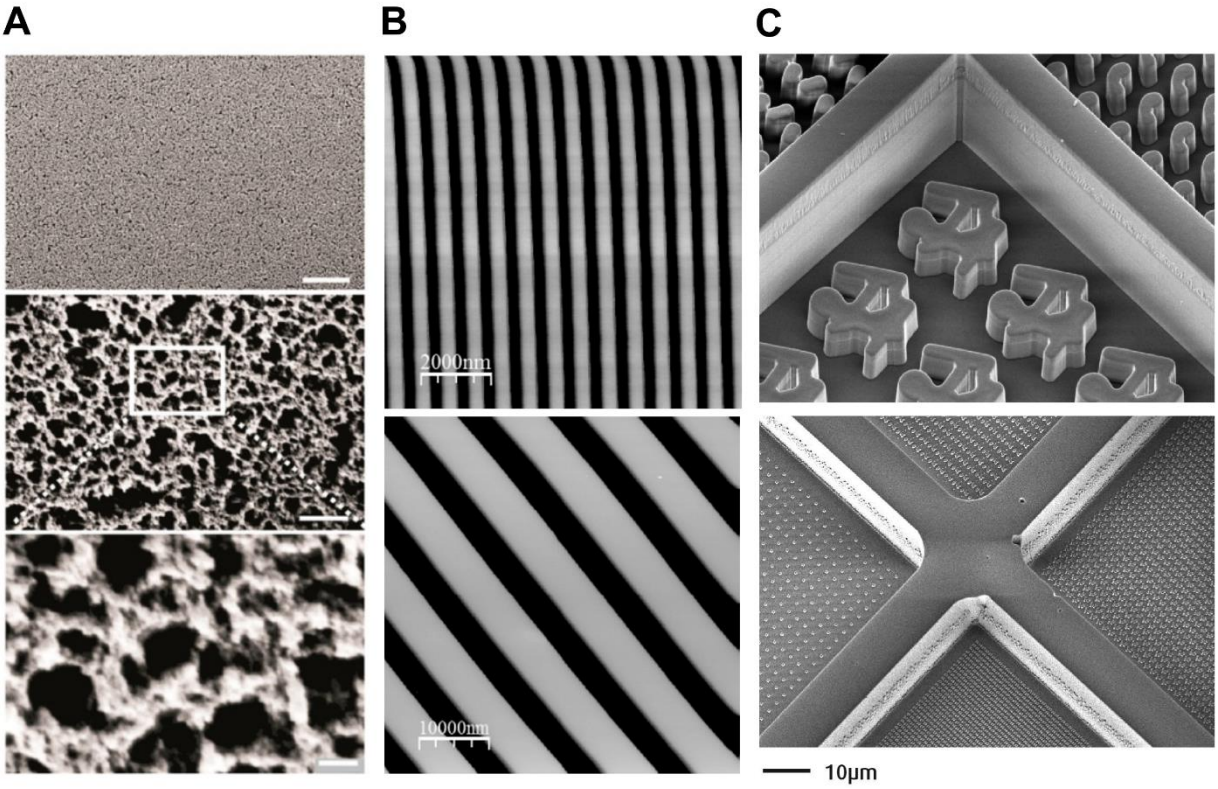

Figure 1: Examples of different surface architectures. A) SEM images of a surface containing roughness levels of 68 +- 30 nm. Scale bars: top image, 5 µm; middle image, 500 nm; bottom image, 100 nm. These hierarchical micro- and nanoroughness levels can promote ESC pluripotency. Adapted with permission from [15]. Copyright (2015) American Chemical Society. **B)** AFM image of groove structures with a groove width of 350 nm (up) and 5 µm (down) known to modulate neuronal differentiation. Adapted with permission from [211]. Copyright (2013) Elsevier. **C)** Upper image represents a SEM image of the TopoChip platform, a high-throughput platform containing 2176 unique micro-structural designs of 10 µm height and separated by walls of 30 µm. The bottom image represents the nanoTopoChip, a high-throughput platform containing 1246 unique nano-structural designs separated by walls of 30 µm. Adapted with permission from [52]. Copyright (2017) Elsevier.

Roughness

Surface roughness can be regarded as topographies with randomly distributed height patterns in micro- or nanometer dimensions. This random feature distinguishes itself compared to other surface types, where the topographical dimensions are precisely controlled. Material roughness is mostly associated with bone tissue engineering and can be introduced to the surface by sandblasting and acid-etching, resulting in superior osteo-integrative capabilities compared to smooth surface titanium implants [10,11]. It is, therefore, not surprising that osteoblast-like cells and MSCs demonstrate improved osteogenic differentiation potential on rough surfaces [12,13]. Also, calcium phosphate surfaces that closely mimic the bone microenvironment, both at a chemical and topographical level, improve the osteogenic potential of MSCs [14] and the osteogenic cell line MG63 [7]. Roughness is utilized for studying other types of cell-material interactions as well. Here, it is interesting to mention that for embryonic stem cells, materials with combined micro- and nanometer roughness [15] or nanometer roughness alone [16] promotes pluripotency. Also, proliferation capabilities can improve on nanorough materials, as shown for endothelial cells [17].

For surface roughness, screening is limited to gradient formats due to their simple design. Through the use of gradients, increased roughness coincides with enhanced proliferation for osteoblasts, while showing the opposite effects for fibroblasts [18]. For osteogenic differentiation, an optimal roughness niche was identified for MSCs [13].

Curvature

Curvature can exist as concave (inward curve) and convex shapes (outward curve). Curvature can influence MSC migration and differentiation [19] and is a useful tool for studying mechanobiology [20,21], since similarities can be found between curvatures *in vitro* and *in vivo* [22]. The effect of curvature on cell behavior is studied in a screening format through the use of wrinkles, for instance, by Zhou and colleagues, who used wrinkles in nanometer dimensions to optimize parameters for osteoblasts attachment [23]. This concept can be expanded in micrometer dimensions and in a 96-well plate format allowing the possibility for combining curvature with different culture media combinations [24]. Furthermore, combinations with other perturbations is achievable through coating wrinkles with, for example, inorganic biocompounds [25].

Grooves

Grooves are continuous lines with variable dimensions across the material surface, which are mainly associated with contact-guidance of cells, i.e., they influence cell orientation. Besides orientation, other cell morphological characteristics such as cell area are affected depending on the proximity and depth of these grooves [26]. In general, grooves can be build in micro- and nano dimensions with varying height profiles, of which both the grooves and ridge length are variable, and even in

hierarchical format combining both dimensions [27]. Grooves can also be placed in perpendicular orientations, which allows the construction of gratings that, depending on the dimensions, gives rise to more complex topographical surface structures.

Microgrooves influence cell behavior in very distinct ways. For example, an increase in global histone acetylation resulted in improving the reprogramming process of fibroblasts towards iPSCs [28]. Grooves influence the differentiation potential of pluripotent cells, with nanogrooves guiding BMP4-induced differentiation of iPSCs [29], the differentiation of ESCs into neurons [30], and the differentiation of astrocytes into glia-like cells [31]. Furthermore, phenotypical characteristics of primary cells can improve on grooves. This is demonstrated by the increased expression of tendon-related genes in tenocytes when cultured on nanogrooves [32]. A similar observation was found with microgrooves, which besides cellular alignment, also aligned collagen-I, the main protein component of the tendon [33]. A similar concept was applied for neuronal cells, where axonal outgrowth orientates according to the grooves direction [34]. Both examples can mimicking the *in vivo* tissue organization, a useful property for tissue-engineering applications.

Because the dimensionality of grooves is strongly variable, screening approaches have been implemented to determine which dimensions are best suited for obtaining a particular cell phenotype. This is illustrated by a screening platform containing 25 units with grooves and ridges in different micrometer dimensions, termed the polyimide (PI) chip. The PI chip was used to identify groove structures that stimulate adipogenic or osteogenic differentiation [26]. The integrated mechanobiology platform (IMP) utilizes gratings and grids in a 96-well plate format, thus enabling the use of molecular biology analysis tools such as qPCR or ELISA. The pitch size of the gratings varies between 500 and 3000 nm, while on the grid geometries the trench width can be varied between 100-300 nm. This platform was used to demonstrate that surface structures can influence IL-2 secretion in T cells, an important cytokine [35]. A screening platform containing both variable micro- and nano grooves is the multi-architectural chip (MARC). It is noteworthy to mention that this platform contains only 18 surface structures, yet besides grooves also contains pillars and pits, thereby creating a broad surface diversity. Surfaces from the MARC were identified that promoted differentiation of neural progenitor cells [36] and ESCs [37] towards either adult neurons or glial cells. Differentiation towards dopaminergic neurons [38] was associated with anisotropic patterns (gratings), while isotropic patterns (pillars and wells) supported glial differentiation.

Complex topographies

Topographies can be designed and produced in increasing complexity at both the micro- and nanometer scale. With complexity also comes larger numbers of potential designs. These designer topographies can, as roughness, curvature, and grooves do, profoundly influence cell behavior, as illustrated by the influence of disordered nano-topographies on MSC differentiation towards the

osteogenic lineage [39]. The height of topographies influences cell phenotype, as shown for nano-topographies with high aspect ratios that support ESC differentiation towards the endoderm lineage in contrast to smaller topographies [40]. Besides enhancing differentiation, pluripotency can also be supported by nano-topographies in honeycomb and hexagonal configurations [41]. These examples demonstrate that a large variation exists in the topographical design space, emphasizing the need for high-throughput approaches to find the most optimal surface structure for a given application.

As a first example, the micro-topographical BioSurface Structure Array (BSSA) contains 504 unique topographical designs with variable spacing between circles or squares, and with variable heights of 0.6, 1.6, and 2.4 µm. This platform has been used to explore the effect on osteogenic differentiation with positive results obtained for an osteoblastic cell line [42] and dental pulp MSCs [43]. Also, topographies were identified that promoted the pluripotency of ESCs [44]. Besides these studies, the BSSA platform found that topographies influence the proliferation of chondrocytes and fibroblasts [45,46].

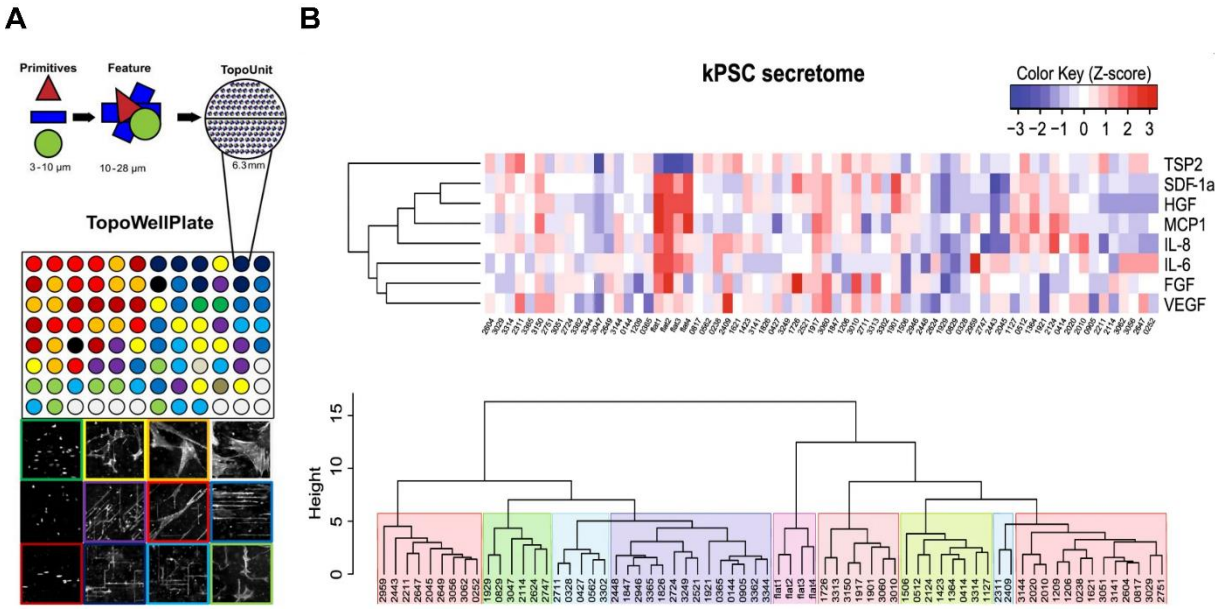

Figure 2: Multiplex ELISA applied in combination with the TopoWell Plate, a high-throughput platform. Applying a multiplex ELISA targeting 8 cytokines and growth factors on this platform allowed inferring if these micro-topographies influence the cell secretome. **A)** The TopoWell Plate contains 87 unique surface topographies and 9 flat surfaces as a control. Seeding kidney derived perivascular stromal cells on these surfaces induces a large variety in morphological characteristics. **B)** Heat map visualization representing the influence of each topography on the expression of these cytokines and growth factors. Through clustering algorithms, micro-topographical surfaces can be grouped based on their secretome profile. Adapted with permission from [54]. Copyright (2018) Nature Publishing Group.

A high-throughput platform designed by our group, known as the TopoChip, is a 2x2 cm^2 platform containing 2176 unique micro-topographies and 4 flat control surfaces [47]. The *in silico* design of these topographies uses three primitives: circles, triangles, and squares. Combining these primitives while varying the number, size, and orientation leads to millions of potential designs. The platform has been used extensively for studying the behavior of cells on micro-topographies while enabling the identification of design parameters associated with a desired phenotype. We identified micro-topographies that promote enhanced clonogenicity of pluripotent iPSCs [48], augment differentiation of tonsil-derived MSCs towards fibroblastic reticular cells [49], improving the osteogenic potential of MSCs [50], or improve phenotypic maintenance of tenocytes [51]. In addition to the TopoChip, a nano-topography version was created with 1246 unique designs [52]. Furthermore, a 96-well platform was developed with each well containing a unique micro-topographical design, enabling other experimental techniques such as ELISA, qPCR or western blot [53]. Combining this so-called TopoWell platform with multiplex ELISA allowed us to associate the secretion profile of mesenchymal and perivascular stromal cells with topographical design and cell shape [54] **(Figure 2)**.

Surface Biochemistry

Cells interact with their surrounding tissue matrix *in vivo*. Some of these interactions are mediated by cell adhesion molecules called integrins, which recognize and bind peptide motifs present in proteins of the surrounding matrix. The RGD sequence is such a well-known peptide motif and is found on multiple matrix proteins, including fibronectin and fibrinogen [55]. Integrins are also capable of specifically recognizing the matrix proteins collagen-I [56] and laminin [57]. Matrix proteins can be presented to cells as a coating and lead to different modes of attachment and signaling. For example, a combination of laminin and poly-L-lysine coating improves the differentiation of PC12 cells towards neuron-like cells [58]. Also, a collagen-I or poly-D-Lysine coating supports pluripotency of ESCs, while laminin or fibronectin activates integrins and downstream pathways associated with differentiation [59].

Besides uniform surface coating, it is possible to create patterned areas with the matrix protein of interest. One strategy is to produce a hydrophobic, cell-repellent surface with islands of matrix proteins, with cells adhering only to protein-containing areas and adjusting their morphology based on the pattern design. The effects of matrix compositions and morphology on cell phenotype can thus be investigated. One of the earliest attempts to utilize this system is from the mid-'90s and involved laminin islands with different surface areas. The authors demonstrated that pattern design influences cell spreading and proliferation [60]. Later, it was shown that the differentiation potential of MSCs is altered when cultured on adhesive islands. Cells grown on smaller patterns had a stronger tendency for adipogenic differentiation, while a larger surface area favors osteogenesis [61]. Besides MSCs, the differentiation potential of other stem cell types, such as epidermal stem cells, can be influenced by utilizing adhesive islands [62].

Due to the large number of matrix components, their possible combinations, and the large pattern design options, high-throughput methods offer an ideal opportunity to find the most optimal biochemical environment. An interesting example is a study where the effects of 32 different combinations of collagen-I, collagen-III, collagen-IV, laminin, and fibronectin on hepatocyte phenotype and differentiation of ESCs towards hepatocyte progenitor cells was determined. The approach found that certain mixtures of ECM compounds had positive synergistic effects on hepatocyte phenotype and ESC differentiation [63]. In **Figure 3 A-C**, we provide the reader with a visual representation of this ECM compound array. In another study, an array of 18 peptide-terminated SAM array elements, each with a unique laminin peptide sequence, allowed determining which sequence is responsible for promoting ESC pluripotency [64]. Besides utilizing matrix proteins, extra complexity can be added by including signaling proteins such as growth factors. This was accomplished on an array platform with 44 different

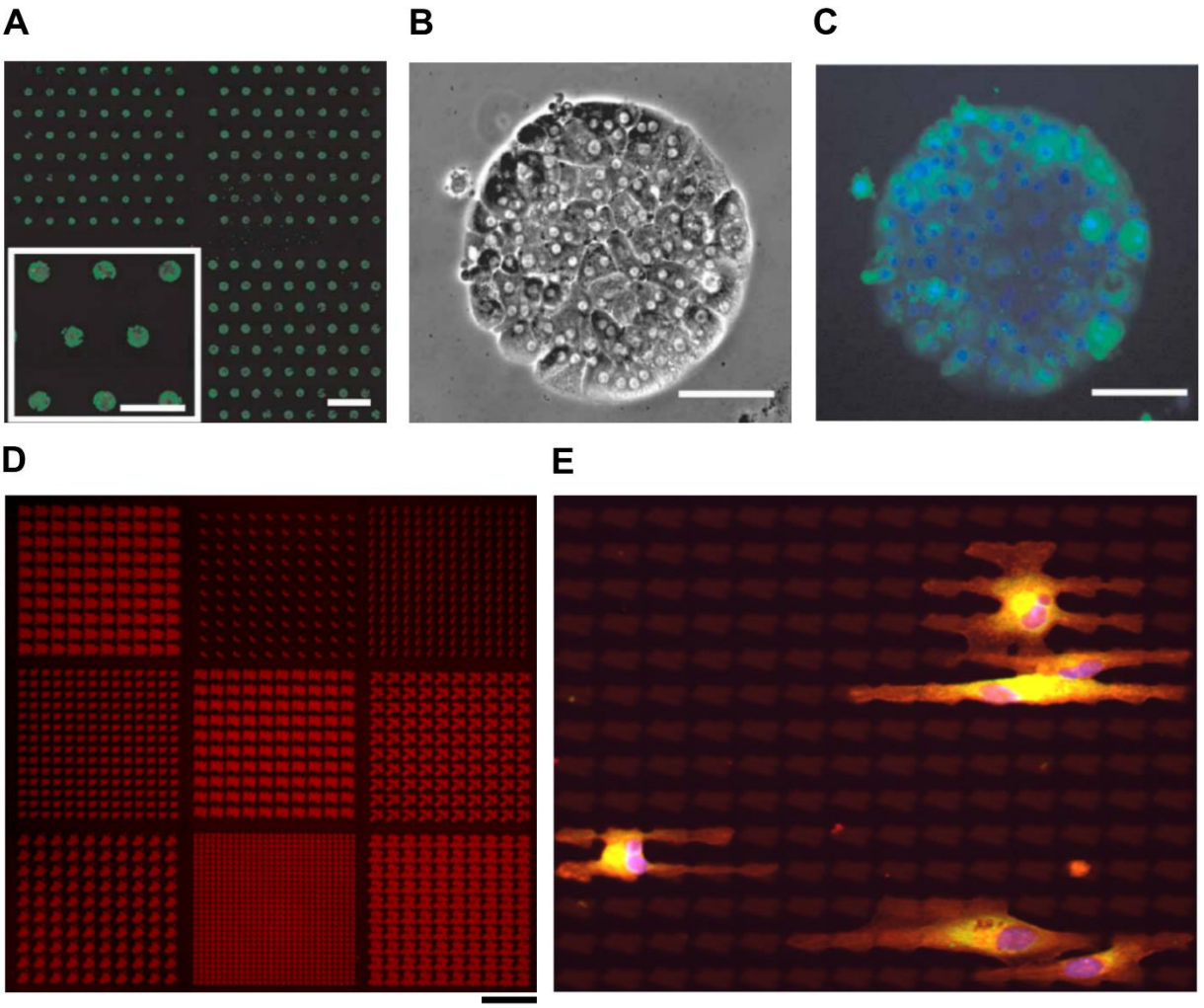

Figure 3: High-throughput screens involving ECM compounds. A) Life/Death assay on hepatocytes cultured on an array of 32 different ECM compositions. Scale bar represents 1 mm. **B)** High-magnification phase-contrast and **C)** Fluorescent image of a single island. Green represents calcein AM and blue the nucleus through a DAPI counterstain. Scale bars represent 50 µm. Adapted with permission from [63]. Copyright (2005) Nature Publishing Group. **D)** RGD islands in a high throughput platform in geometric shapes of varying parameters. The design is based on a mask for creating the TopoChip platform. Scale bar represents 100 µm. **E)** CellPaint assay on BM-hMSCs grown on this substrate allows studying the influence of different densities of RGD islands on cell morphology in a high-throughput and high-content format (picture courtesy of Urandelger Tuvshindorj from the MERLN Institute, Maastricht University).

combinations of signaling proteins, on which ESC neurogenic differentiation was investigated [65]. In a similar study, an array of 25 different substrates was used to find that the effect of growth factors was modulated depending on the underlying matrix compositions [66].

The examples above illustrate the usefulness of screening matrix compounds, especially in combination with soluble cues. Concerning the dimensions of these adhesive islands, we reason that varying this in a high-throughput matter can be of substantial biological importance, especially when including different matrix compounds are included. Research in this niche can easily be accomplished by utilizing the same lithographical masks for the fabrication of other high-throughput biomaterial technologies. We recently developed such a high-throughput design with RGD peptides based on the TopoChip design **(Figure 3 D-E)**.

Surface Chemistry

Surface chemistry has a strong effect on cell behavior and can be used to endow medical implants with specific bio-active properties. However, the relationship between surface chemistry and cell response is difficult to model. Therefore, high-throughput strategies to study the effect of surface chemistry on protein adsorption or cell function are of great interest. In cell culture, surface chemistry has a strong effect on cell behavior. Standard cell culture is carried out on tissue-culture plastic, which is an oxygen plasma-treated polystyrene material. Oxygen treatment changes the chemistry of the material by incorporating oxygen radicals, which hydrophilizes the surface, thus improving cell-substrate attachment [67], cell-cell contacts [68], and proliferation [69]. Through lithography, this concept can be implemented for creating shapes that facilitate cell attachment [70,71]. Also, gradients can be produced to find the most optimal oxygen incorporation and roughness level for a particular phenotype [72]. The link between surface chemistry and the response it elicits on cells may be through differential deposition of serum matrix proteins such as fibronectin that adsorb on the substrate [73]. Surface chemistry can change the conformational structure of fibronectin, which in turn affects the binding affinity to integrins and thereby influences cell adhesion [74]. Nevertheless, surface chemistry might affect cell behavior directly through new and unknown mechanisms or mimic the effect of biological molecules, similar as seen with small-molecule screens.

A large variety of monomers exists, the building blocks of polymers. These monomers can be combined through chemical reactions into various polymers with different chemical and physical properties. The amount of possible polymer variation is enormous, which is illustrated in a high-throughput study where 576 novel polymers were created by different combinations of 25 monomers, each carrying the same chemical acrylate backbone [75]. Besides acrylates, other polymers exist that are popular for biomedicine applications such as polyesters and polyurethanes (PU), which are biocompatible and biodegradable. For PU, a polyurethane library was created with 278 different glycol backbones for studying their effect on wettability [76]. A similar approach was utilized with 44 different

poly-acrylates for determining their affinity with fibrinogen [77]. An overview regarding the different polymers used for biomedical applications and their advantages and disadvantages is excellently reviewed elsewhere [78].

The previously presented examples did not involve cell-based experiments. Cell behavior can give a more accurate representation of the *in vivo* properties of the surface chemistry on tissue engineering constructs and medical devices by measuring properties such as toxicity, adhesion, and matrix deposition. For example, by utilizing 60 different polymers based on different combinations of polyurethane, polyols, diisocyanates, and variable chain extenders, their compatibility with epithelial cell adhesion was determined [79]. Also, in an extensive high-throughput manner involving 1152 different polymers, the adhesion properties of these polymers against MSCs, neuronal stem cells, and chondrocytes were studied [80]. In this study, only 24 polymers were blended, including PGLA and PLA, which are frequently used in regenerative medicine. Cell adhesion of suspension cells can also be accomplished through polymer coatings, as demonstrated in a study utilizing a library of 210 different polyurethanes and 58 polyacrylates. Here, the authors identified polymers that promoted adhesion and proliferation [81].

Polymer composition can be also be used to control specific cell behavior *in vitro*, e.g., to improve proliferation or stem cell differentiation [82]. We mentioned before the construction of a library of 576 polymers based on 25 different acrylate monomers [75]. The same library contained chemical compositions promoting endothelial differentiation of ESCs [83]. Utilizing different blends of PDLA and PCL, both FDA approved biomaterials, it became possible to influence ALP levels of two osteogenic cell lines [84]. In a library of 120 varieties of polyurethane, polymers were identified that enabled the preferential binding of an MSC subpopulation with increased osteogenic potential [8]. Through a library of 141 homopolymers and 400 co-polymers, the effect of these substrates on dental pulp stem cell differentiation was assessed [85]. Of interest, the authors managed to predict the behavior of these cells on the polymers tested through computation models. Polymers also allow the phenotypic maintenance of primary cells, as demonstrated by a screen utilizing a library of 380 different polyurethanes and acrylates [86].

Chemistry can influence the phenotypical maintenance of ESCs, as demonstrated in a study applying 496 polymer blends based on 22 different acrylate combinations [87]. Through in-depth characterization of polymer properties, such as wettability, roughness, and elasticity, associations were made with cell phenotype. In **Figure 4**, we provide the reader with high-throughput data visualization from this study. Furthermore, they found that vitronectin from the culture media adsorbed to the polymers, and resulted in a specific integrin-binding, which initiated the cell signaling that promoted pluripotency. In parallel with the study, this research group studied embryoid body adhesion on the same

polymer array. Of interest is that here both the pre-adsorbed fibronectin and the bare polymer were responsible for controlling cell adhesion [88].

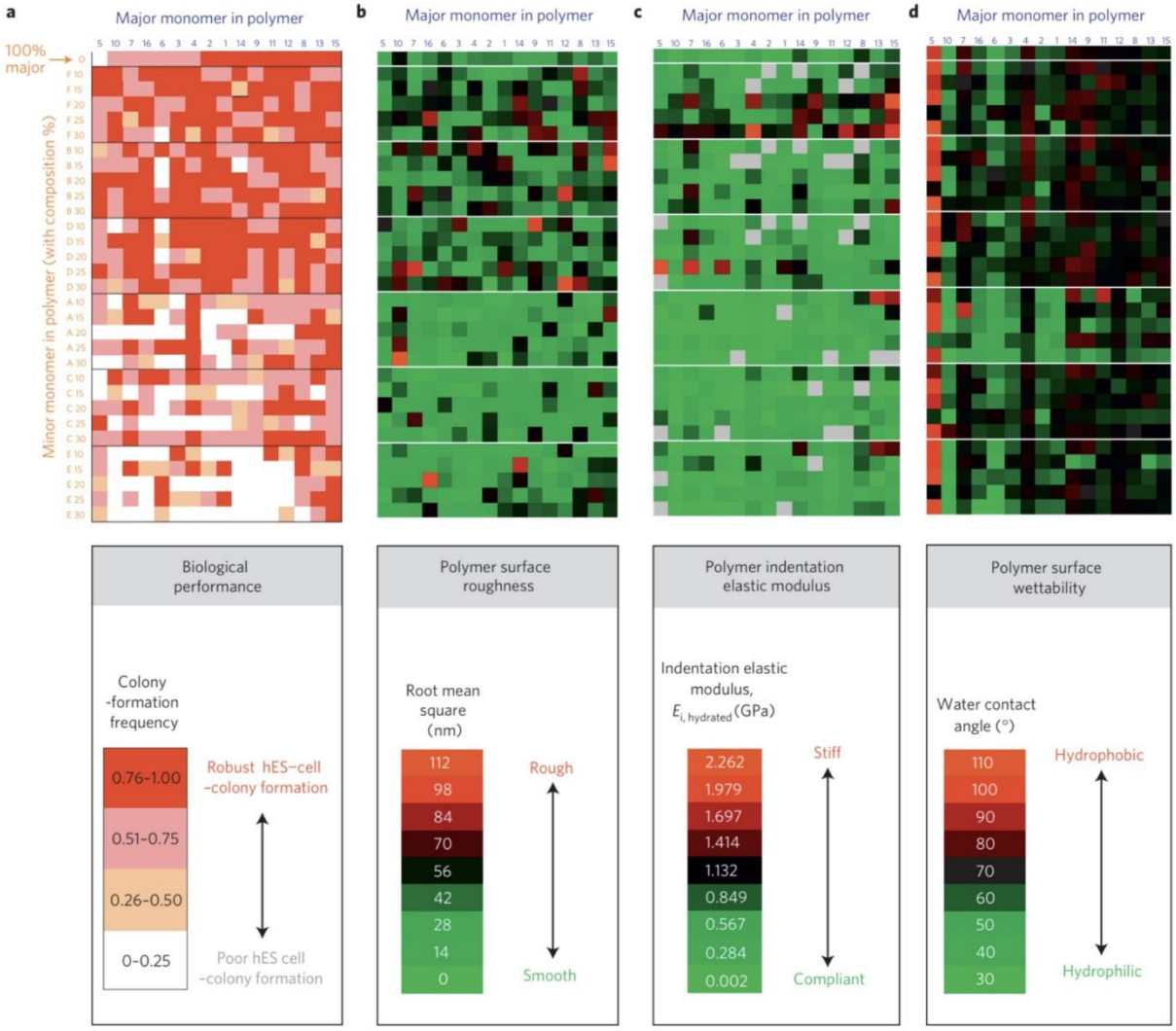

Figure 4: Example of a visualization of a high-throughput platform mapping the biological response of ESCs against 496 different polymers. Through measuring surface roughness, elasticity, and wettability, functional relationships between surface characteristics and cell phenotype can be measured. Here, a positive relationship between ESC colony formation and moderate wettability was established. Adapted with permission from [87]. Copyright (2010) Nature Publishing Group

Another clinically relevant application are polymers with properties that prevent implant infection. Based on the previous library for studying the behavior of ESCs and EB's, structurally related polymers were identified that resist bacterial attachment, which was further validated by *in vivo* testing [89]. Follow-up studies demonstrated a clear relationship between the chemical composition of the polymers and antimicrobial properties [90]. Also interesting to mention is that the same group applied a "multi-generation" screening, whereby first homopolymers from a library of 116 acrylate monomers were identified that resist antibacterial attachment [91]. Afterwards, these hit monomers were mixed in polymer format to conduct a second screen, after which hit polymers were selected to make composite materials.

Until now, we focused on chemical characteristics that influence protein adsorption, cell behavior, and microbial attachment. However, in the context of medical implants, degradation, durability, and physiomechanical properties are relevant parameters for clinical performance as well. Assessing these characteristics in a high-throughput context is a challenging endeavor, which Kohn and co-workers achieved by simultaneously assessing the polymer structure of 144 polymers, their glass transition temperature, hydrophobicity, mechanical properties, and fibroblast proliferation [92].

Hydrogels

Hydrogels are a popular tool for guiding cell behavior through the possibility to simultaneously control physical, chemical, and biochemical parameters. The main difference between the previous paragraphs is that hydrogels can provide a 3D environment, thereby more closely resembling the *in vivo* context of some tissue types. In hydrogels, molecules for cell signaling can be attached to a flexible backbone with dynamic physical properties. This allows regulating the stiffness of the gel, which is a crucial regulator of cell behavior, as demonstrated by the landmark paper of Disher and co-workers [93]. In this study, hydrogels that match tissue elasticity drives MSC differentiation towards the matching cell types. Also, for pluripotency of stem cells, the stiffness of the surrounding environment can be a crucial factor [94].

Since parameters such as biodegradability, biomolecule presentation, growth factor release, and mechanical properties can be varied, high-throughput approaches help determine the most optimal parameters for controlling cell fate in hydrogels. This is demonstrated by a microwell platform with modular stiffness, where individual microwells can be functionalized with a different protein combination [95]. Environmental niches promoting the differentiation of MSCs and the self-renewal of neuronal stem cells were discovered with this platform. This concept was further expanded by fluctuating stiffness levels, gel degradability, cell density, ECM compounds, soluble factors, and cell-cell interaction components, thereby creating more than 1000 different niche environments that were assessed on their potential for controlling ESC pluripotency [96]. Also, combinational arrays can be generated where polymer concentration, peptide presentations, and growth factor concentrations are varied. This allowed the identification of an optimal niche for myofibrogenesis in human mesenchymal stromal cells [97]. The same group further demonstrated that also mechanical stimulation can be applied on hydrogels in an array format, whereby implemented sensors allowed monitoring the progress of hydrogel stiffness changes in real-time [98].

Other material fabrication parameters that can be controlled in hydrogel synthesis are monomer blending, pH, and crosslinker concentration. In an array system, 80 different polymer blends where combined resulting in gels with different stiffness and elastic properties [99]. Thermo-responsive properties are interesting for clinical applications because they can be used to release cells from the hydrogel, for example, after injection. A high-throughput screen for identifying thermoresponsive

hydrogels was performed by Zhang and colleagues. The authors tested 2280 different polymer compositions and identified hydrogels with optimal properties for cell attachment and temperature controlled release [100].

An exciting opportunity for clinical application is the use of hydrogels in microbead format. Due to the small size of these beads, nutrient and gas exchange is facilitated, while cells are in direct contact with a physiologically relevant matrix. In this context, the optimal elasticity of agarose-based microbeads was identified using a high-throughput approach [101]. Similarly, a high-throughput screen identified optimal parameters for an MSC and hepatocyte co-culture inside alginate-based microbeads [102]. This study further found improved liver enzyme levels after implanting these co-culture microbeads in rats, suggesting that the approach does have potential clinical applications in the future for restoring tissue and organ function.

Micro-Fluidics and Droplet Technologies

Microfluidics is defined as the control of fluids in micrometer dimensions. By working in these dimensions, microfluidics enables the control of experimental parameters in the cell size range. Due to these small dimensions, microfluidics come hand in hand with lab-on-a-chip technology and hold the promise of influencing a large number of parameters on a small platform. The architecture of the microfluidic platform is modifiable and allows, for instance, dynamic control of growth factor or cytokine gradients [103]. Furthermore, it is possible to apply different surface (bio)chemistries [104] and surface structures [105] inside the platform. Some platforms have included stretching as a biological signal mimicking *in vivo* conditions [106]. An extra layer of complexity can be introduced through compartmentalization, in which different separate cell systems are connected, which moves the platform more towards an organ-on-a-chip concept. These examples demonstrate that the microfluidic lab-on-a-chip concept is a highly versatile and attractive platform for high-throughput research in a regenerative medicine context [107].

Micro-fluidics research in a high-throughput setting often involves the use of compound gradients. For instance, drug screening was performed on cancer cells to asses their effect on migration kinetics [108]. In a similar approach, Zhang and colleagues utilized 3120 microchambers to monitor migration in combination with anti-metastatic drugs [109]. In a tissue-engineering context, micro-fluidic constructions also made it possible to generate growth factor gradients to study the differentiation of neural stem cells [110,111]. In a 3D mesenchymal stem cell culture, growth factor gradients with the most optimal concentration of TGF-β1 to induce chondrogenesis were identified [112].

An emerging technological micro-fluidics application is the use of droplets that enable high-throughput analysis at the single-cell level. The technology is compatible with single-cell omics, which is highlighted by a study with embryonic stem cells where the early onset of differentiation was studied in droplets containing lysis buffer, reaction mix, and barcoded primers [113]. Other applications and

techniques concerning droplet-based microfluidics for single-cell omics are excellently reviewed elsewhere [114].

Small Molecule Screens in Regenerative Medicine

Libraries of bio-active compounds are a useful high-throughput asset in the field of regenerative medicine to fine-tune growth and differentiation conditions of cultured cells. For instance, compounds targeting pluripotent stem cell viability were identified in a screen utilizing approximately 52,000 compounds [115], which can be applied to eliminate undifferentiated stem cells before implantation. For directing cell fate, high-throughput screens are a useful tool to identify novel compounds for stem cell differentiation or phenotypical maintenance. For example, in a screen utilizing 4000 compounds, two small molecules were identified that allowed 80% of ESCs to differentiate towards the endoderm lineage, superior to the commonly used proteins Activin A or Nodal [116]. Also, ESC neuronal differentiation is inducible through small molecules, as shown in a study employing over 100,000 compounds [117]. For MSCs, high-throughput compound screening can be useful to identify molecules that improve MSC differentiation potential. In a study with a library of 1280 small molecules, novel compounds were found that improved the osteogenic differentiation of MSCs with equal efficiency as reference osteogenic molecules such as dexamethasone, vitamin D3, and cAMP [118]. In standard conditions, ESCs are cultured on a fibroblast feeder layer and in the presence of serum. The presence of xenogenic compounds limits clinical application due to potential immunological host reaction, which is why researchers try to define a chemically-defined media composition. In this context, a high-throughput screen with 50,000 compounds resulted in a culture of pluripotent ESCs without a feeder layer, serum, and LIF [119].

Besides directing cell fate, small molecules are also useful to improve matrix deposition. Through a screen of 1280 small molecules, compounds were identified that improved the development of a collagenous-rich matrix in the pre-hypertrophic chondrogenic cell line ATDC5 [120]. These small molecules offer translational perspectives for bone tissue engineering by utilizing them in allografts for promoting endochondral ossification. Through applying the same library, compounds were identified that mimic hypoxia, resulting in increased secretion of VEGF in MSCs [121]. These compounds can have useful tissue engineering applications because VEGF secretion stimulates blood vessel formation.

The Screening Toolbox

The use of materials to support missing or diseased tissues is not a novel concept. Evidence suggests that the ancient Mayans used nacre shells as a biomaterial to replace missing teeth [122]. Similarly, archeologists found clues that inhabitants of the ancient Roman Empire applied iron as tooth replacement [123]. Other evidence exists that in ancient Egypt inhabitants carried prostheses [124]. In present times, biomaterials are very important for a large group of patients, where titanium hip replacements,

stents for obstructed blood vessels, or hemodialysis devices for blood purification can be regarded as significant achievements in the field. In the previous section, we discussed how the properties of materials could be altered to control their bioactivity. Next, we will discuss the technologies needed to engineer these materials.

Micro- and Nanofabrication of Surface Architectures

Lithography and Hot Embossing

Multiple methodologies exist to fabricate micro- and nanopatterns. In **Figure 5**, a schematic overview illustrates the methods we used to construct micro-topographies of the TopoChip platform [47,125], which is a good example of the different steps to come from design to the final material. First, a mask is produced based on a design, which is subsequently used to produce a mold using the technique of lithography. It involves the use of a sturdy and hard substrate such as silicon or nickel, coating with a photoresist, and shining light through the mask. This mask design corresponds with the topographical pattern, with the passing of UV light subsequently dissolving the underlying photoresist. Next, acid etches the material while leaving the photoresist intact. The duration of the etching step determines the height of the surface structures. After the creation of the mold, the patterns are transferred to a new material that is either photo- or heat-curable. A commonly applied material is the heat-curable polymer polydimethylsiloxane (PDMS) that requires a chemical initiator to harden over time. Typically, PDMS with the initiator is poured over the master mold and fills the pattern cavities. After hardening, the PDMS is peeled off, containing the replica patterns. PDMS can be used directly for cell-based experiments [126] and is a favorite tool in the microfluidics research field due to its high fidelity for pattern transfer and excellent optical properties. Nevertheless, PDMS is chemically very different from polystyrene, the golden standard for cell culture, which makes it difficult to compare research results [127]. Therefore, patterns can further be transferred into secondary and even tertiary substrates, eventually also into polystyrene.

Another popular method to transfer imprints into another material is through hot embossing. Here, the material temperature is increased beyond the glass transition temperature, causing it to soften. By applying pressure, patterns are transferred from the mold to the polymer. After cooling, the material is peeled off the mold. Hot embossing is not compatible with every polymer. For instance, direct embossing of polystyrene on a glass waver results in breaking or deforming either the waver or PS due to high demolding forces [125]. It is possible to directly apply hot embossing on a PDMS substrate [128]. However, the pressure might damage the PDMS imprints in the long term. Therefore, as shown in the scheme, we used an intermediate between PDMS and PS, called Ormamold, to transfer the imprints. Here, the Ormostamp is photo-cured through UV radiation, polymerizing the monomers into a hard substrate that carries the negative imprint. The same principles also allow the transfer of nano-patterns with high fidelity [52]. Besides PS, many materials are compatible with hot embossing, making this a

highly versatile method for fabricating surfaces, also in an industrial setting [129]. The photo-curing concept to generate Ormostamps can also be applied in a wide variety of tissue-engineering applications. The technique can be harnessed for tooth replacement materials [130], and cell culture applications such as the generation of scaffolds [131]. Also, for hydrogels, photocuring is very popular due to the possibility to regulate physical behavior dynamically. We refer the reader to a recent review that provides a detailed description of these applications [132].

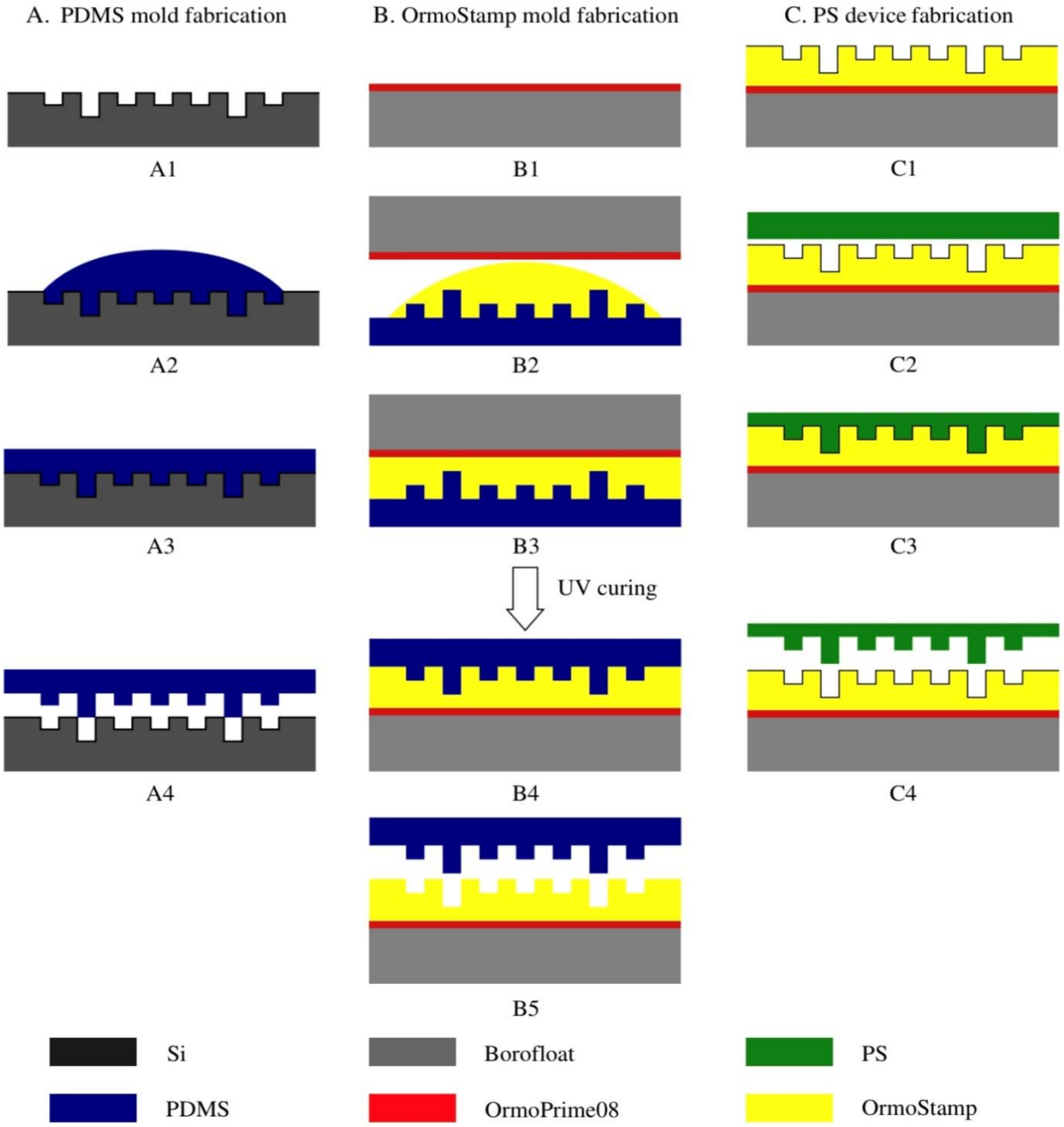

Figure 5: Schematic overview for micropatterning stiff and brittle polystyrene. Due to the high demolding forces required to remove PS from the Si waver, extra steps through a OrmaStamp intermediate facilitates the transfer of the micro-patterns. **A)** PDMS heat curing and demolding on a silicon waver. **B)** Ormostamp mold fabrication involving UV curing on the PDMS stamp. **C)** PS hot embossing on the Ormostamp. Adapted with permission from [125]. Copyright (2017) Elsevier.

Besides hot embossing, other specialized thermoforming techniques exist. For example, for creating COC microwells inside a screening plate, pressure through an inert gas is applied in combination with heating of the material [133]. Another alternative is injection molding, whereby heated material is directly injected in a mold. This technique finds applications in creating biomaterials such as micro-fluidic platforms [134]. A detailed review of the advantages of these methods are reviewed elsewhere [135].

Protein and Chemical Patterning

Microcontact Printing

Proteins or polymers can be printed onto surfaces in any desired pattern. A commonly applied method to accomplish this is through micro-contact printing. As we explained previously, through lithography techniques, a PDMS stamp with surface structures can be generated. Such a stamp is employed for transferring either matrix proteins or chemicals to a new substrate. Patterns are thus generated when only the elevated PDMS regions come into contact with the substrate. Pattern transfer can be accomplished directly, for example, by coating a PDMS substrate with laminin, after which the laminin is transferred to another substrate by bringing the substrate into contact with PDMS. Such an approach allowed the generation of adhesive islands and subsequent cell patterning in a microfluidic chamber [136]. A more indirect, yet commonly applied strategy, is creating hydrophobic and hydrophilic regions that either allow or disallow protein adsorption. A chemical used to produce these regions can be alkanethiol, which forms self-assembled monolayers (SAMs) on gold [137]. Alkanethiols transfer to the PDMS stamp when dipped into a solution. When the PDMS stamp containing dried alkanethiol comes into contact with a gold substrate, SAMs on this gold substrate will form according to the pattern present on the PDSM stamp. After exposure to a second type of alkanethiol, new SAMs will form between the first SAM patterns. Because end groups on the alkanethiols determine their protein adsorption affinity, patterns of adhesive and non-adhesive regions are created. For instance, methyl groups favor the attachment of proteins, while SAMs with ethylene glycol resist protein adsorption. We provide the reader with a schematic representation in **Figure 6**. Deviations in these chemistries are common, yet the same principle concerning the use of a stamp is applied. This is demonstrated in a study documenting improved keratinocyte differentiation through adhesive islands [62]. A substantial advantage of the technique is that it allows creating polymer patterns at sub-100 nm resolution [138]. Furthermore, considerable flexibility exists in the viscosity and type of ink chemistry used in the setup, which typically already contains polymers through a mixture of monomers and initiators. For example, light-emitting diodes can be created by stamping a conductive polymer solution [139]. Even the construction of topographical structures is possible through a combination of polymers and inorganic chemistry [140,141]. For a detailed documentation of the wide variety of micro-contact printing applications, we refer the reader to specialized reviews [142–144].

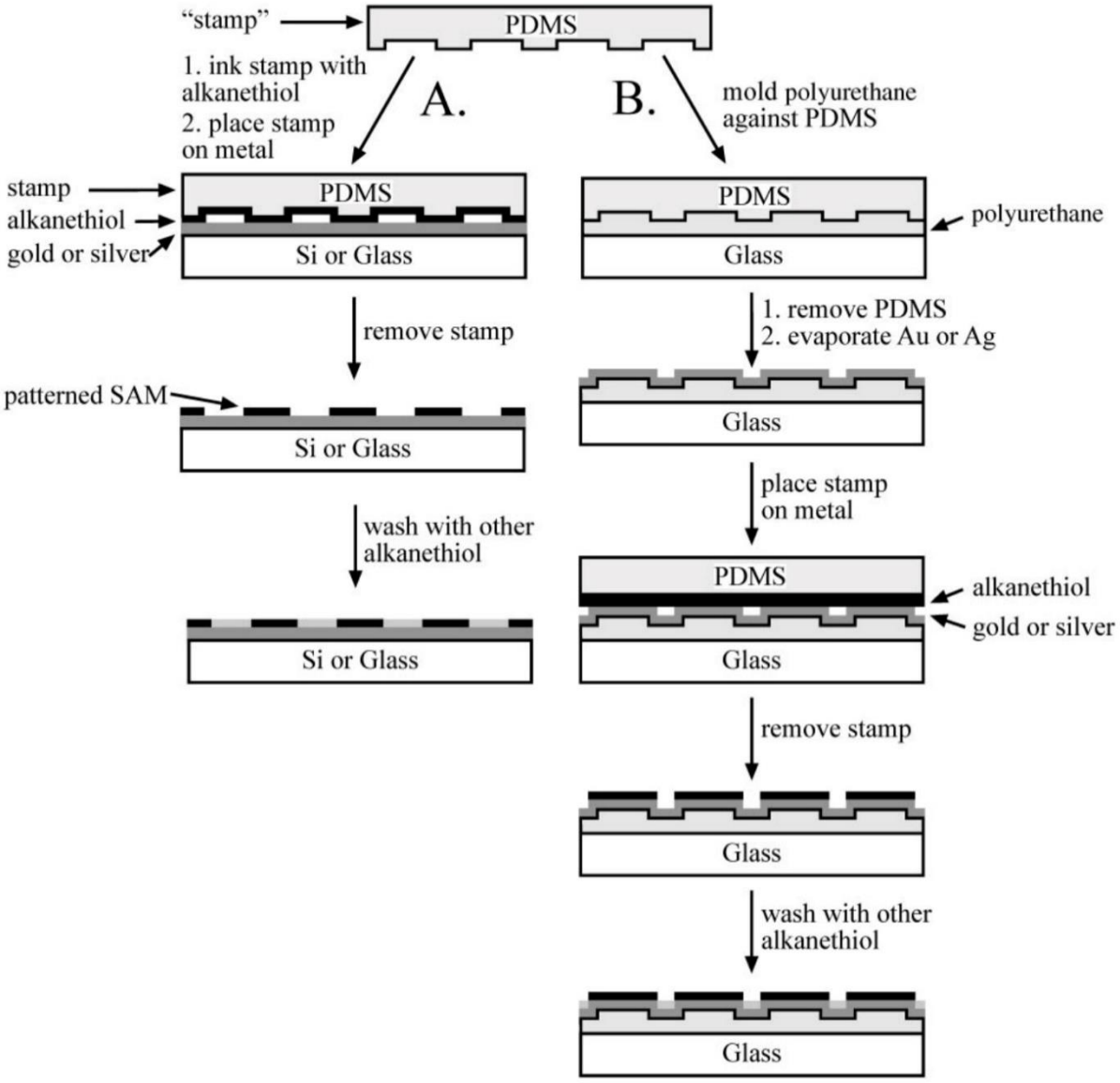

Figure 6: Schematic overview for micropatterning proteins. A) A stamp is inked with an alkanethiol and placed on a gold surface; the pattern on the stamp is transferred to the gold by the formation of an SAM on the regions that contacted the substrate. The bare areas of the gold are exposed to a different alkanethiol to generate a surface patterned with a SAM that presents different chemical functionalities in different regions. **B)** The PDMS stamp can also be used as a master to mold harder polymers and generate contoured surfaces. After evaporation of a layer of gold, these surfaces can be functionalized by μCP of one alkanethiol with a flat stamp. The grooves of the substrate can then be exposed to an alkanethiol presenting a different functional group to produce a contoured surface with patterned chemical reactivity. Adapted with permission from [137]. Copyright (1999) Elsevier.

Inkjet Printing

A disadvantage of microcontact printing is that it requires the fabrication of a lithography mask to construct the patters of the stamp. This is time-consuming and also reduces flexibility if new patterns need to be generated. An attractive alternative in this regard is the use of inkjet printers. Here, primary monomers are typically first printed, after which a second monomer or initiator is mixed with the first monomer, allowing *in situ* polymerization of the monomers [145]. The technique, therefore, not only allows

flexibility in pattern design, yet can also create a broad polymer diversity making this ideal for high-throughput studies. For example, inkjet printing allowed designing 2000 different hydrogels, of which their functionality was analyzed for cell adhesion and thermos-responsive release [100], and for screening 380 different polyurethanes and acrylates for inducing a hepatocyte phenotype [86]. Deviations usually exist by altering the surrounding environment during the printing process. Polymerization reactions can be inhibited when oxygen is present, or slow down the polymerization reactions, causing the formation of irregular spots. These considerations were taken into account in studies utilizing the printing of hundreds of polymer spots for ESC differentiation [83] and antibacterial attachment [89] by utilizing an argon atmosphere and a UV lamp to increase the polymerization speed. A disadvantage compared to microcontact printing are restrictions in the physical parameters of the chemical, such as high viscosity levels [146].

Photopatterning

Lithography can directly pattern polymer surfaces, a method that does not require etching of a mold. For example, exposure of surface-bound benzophenone to UV light enables stable binding with target molecules [147]. Through this method, matrix proteins are covalently bound to the surface for cell adhesion experiments. Previously, we have shown that the use of photoresists is useful for micro-patterning, and the same principle can also be utilized for protein patterning when the resist adsorbs proteins. Photomasks give precise control of the desired pattern and are also applicable for high-throughput purposes without the need to fabricate a stamp such as in microcontact printing [148].

Computational Techniques

High-throughput experiments are characterized by generating massive amounts of data. To mine this wealth of data, know-how is needed to process data correctly. In this time of big data, the need to handle it increases, and fortunately, more and more user-friendly bioinformatics tools exist to process them. Computer languages such as R [149] and Python [150] are becoming more accessible, thanks to interfaces such as R Studio [151] and Spyder. Also, numerous online learning platforms such as Edx (https://www.edx.org), Coursera (https://www.coursera.org), and DataCamp (https://www.datacamp.com) offer basic and advanced bioinformatics courses. For high-throughput imaging experiments, which can quickly amount to thousands of images, user-friendly software such as Cellprofiler and Fuji exist for handling large quantities [152,153]. Machine learning algorithms to correlate the experimental design variables to phenotypical outcomes can be handled by software such as Rapidminer [154]. In this chapter, we provide the reader with an overview and description of how these computational techniques facilitate the analysis of high-throughput data.

Batch Effects

Data derived from high-throughput technologies is prone to batch effects due to data retrieval from multiple time points or different experimental conditions. This leads to technical variations in the data, resulting in biases and misleading conclusions. Batch effects can occur through the performance of experiments by multiple operators, the use of different laboratory equipment, and variations in serum or growth factor batches and other reagents. Biological factors can also play a role. For example, the use of different stem cell donors can influence experimental outcomes, as illustrated by Siddappa *et al.*, demonstrating that the differentiation potential of MSCs can vary between donors [155]. Although batch effects can occur in any experimental setup, finding batch effects is easier for high-throughput and high-dimensional data. Examples of the identification of batch effects in scientific studies are found in an interesting review by Leek *et al.*, where methods are described to correctly handle data influenced by batch effects [156]. An example of such a method is surrogate variable analysis, which demonstrated its usefulness for overcoming heterogeneity in gene expression studies [157]. Also, batch effects in high-throughput applications can be identified by machine learning techniques like clustering analysis and PCA, which will be discussed further.

Image Processing

Imaging is a particularly suitable technique for obtaining high-throughput data and is facilitated by microscopes that can take thousands of images in a matter of hours. Our group applied this technique multiple times on the TopoChip platform that contains a total of 4352 topographical units on a 2 cm^2 surface [49,51,158]. A limitation is that usually, only a few proteins are targeted due to the spectral overlap of the applied fluorochromes. However, for improving the information content of images, techniques such as CellPaint allow staining multiple cell organelles besides the classical nuclear or actin staining [159]. To analyze the large number of images that are typically generated, software scripts such as in Matlab can identify and quantify both cell morphology and intensity features of the images [47]. However, also open access software such as CellProfiler allows image processing both in 2D and 3D while enabling the extraction of highly dimensional data [160]. Examples of applications include the segmentation of nuclei and quantifying DNA content in an RNAi library screen [161], or measuring protein levels in both the cytoplasm and the nucleus during differentiation events [162]. Also, in immunohistochemistry images, CellProfiler identified CD4+ and CD8+ T cells in human tissue samples [163] and quantified the amount of CD4+ cells in patients with chronic graft-versus-host disease for determining disease severity [164].

The algorithms that allow pattern recognition are continuously improved. A promising and emerging strategy in this regard is the use of deep learning algorithms. This machine learning approach allows superior nuclei segmentation across multiple image types [165,166]. Furthermore, it can be applied in a high-throughput context for identifying cellular phenotypes [167]. In the clinic, deep learning algorithms are beneficial for the automated detection of acute lymphoblastic leukemia cells [168], tumors [169], and polyps [170]. Since the creation of these scripts requires a specialist to develop them, the application

by biologists and clinicians is typically performed through software such as U-Net [171]. CellProfiler also offers modules for applying pre-trained neural network models for cell segmentation [172], assessing the quality of images [173], and tracking cells during live-cell imaging [174]. In the future, more of these algorithms will become available, which, in combination with user-friendly software, will further increase the possibilities and quality of image-based studies. We further refer to two recent reviews that describe in detail the use of deep learning for cellular imaging [175] and medical image analysis [176].

Machine learning

Besides applying deep learning in imaging studies, also other machine learning algorithms are useful in a high-throughput context. For example, when we would like to understand which and how strong experimental variables contribute to an observed effect. This effect can be a phenotypic condition, with the input parameters being a wide variety of different materials or polymers. Through machine learning, meaningful relationships between input and output variables can be identified and visualized with the possibility to predict outcomes. Furthermore, machine learning approaches such as PCA allows dimensionality reduction, thereby enabling to filter out irrelevant data from datasets. In this section, we describe how machine learning algorithms benefit high-throughput data analysis. We also refer to a recent review from our group on the use of machine learning algorithms in a biomaterial context [177].

Regression Analysis

A classical machine learning approach for measuring cell-material interactions is through linear regression. This method employs a best-fit line whereby the distance between the actual and predicted measurements is minimized. This allows determining and quantifying significant correlations between the input (independent) and output (dependent) variables enabling the prediction of outcomes **(Figure 7A)**. More complex methodologies exist, such as multivariate linear regression with more than one independent variable. The following examples show how regression models are useful for regenerative medicine applications. A regression method was used for inferring if the output from magnetic resonance imaging correlates with glycosaminoglycan content of different engineered cartilage constructs [178]. Through multivariate linear regression, optimal polyurethane compositions were identified against microbial attachment [179]. Similarly, regression models allowed identifying the effect of antibacterial attachment of ions in a polymer array [89].

Classifier Algorithms

For some applications, it might be important to classify observations according to specific criteria. This is useful for determining if an email should be classified as spam, or for identifying plant species based on a picture alone [180]. Here, classifier algorithms are trained for determining which characteristics correspond best with a specific category. Usually, two subsections of the data are taken, one for training the classifications and one for evaluating the performance of the classifier. Many

classifier algorithms exist; these include k-nearest neighbors [181], random forests [182], support vector machines (SVM) [183], and the before mentioned deep learning [184]. These algorithms are particularly well suited for high-throughput applications. For example, besides useful for image processing, deep learning classifiers allowed modeling and predicting which polymer characteristics are associated with embryoid body cell adhesion [185]. In our group, we applied random forest algorithms for identifying which topographical features are associated with a particular phenotype **(Figure 7B)** [48,50,51].

Cluster Methods and Dimensionality Reduction

For understanding and visualizing complex data acquired from high-throughput experiments, clustering analysis is an essential computational approach. This method groups data points based on similarity and is therefore useful for identifying surface structures or polymers with similar or unique effects on cell behavior. An example of such a cluster method is called k-means clustering [186]. k-means is a relatively simple algorithm adapted in many scientific disciplines. Applications include grouping differentially expressed genes together to allow visualizing and identifying genes associated with the different developmental stages of the kidney [187]. Similarly, in embryonic stem cells and trophoblasts, genes associated with pluripotency and lineage specificity can be clustered and distinguished [188]. However, k-means suffers from some drawbacks, since the user has to choose the number of clusters beforehand, leading towards potential biases. Furthermore, highly dimensional data is challenging to analyze through the k-means method as well as for similar clustering approaches such as fuzzy c-means [189].

An alternative is hierarchical clustering. Here, all data points are split into two clusters that share the least similarity based on Euclidian difference. This process is repeated until each data point is divided into a cluster, creating a tree-like graph. We previously mentioned the TopoWellPlate, where the influence of a large variety of surface structures on the secretome of MSCs was investigated [54]. Through hierarchical clustering, we grouped surfaces from the TopoWell plate that exert similar or unique effects on the secretome profile of MSCs. In a similar approach, yet with polymers instead of surface structures, and microarray data instead of multiplex ELISA, the effect of different polymers on gene expression profiles in MSCs was assessed through clustering [190]. Multiple variations in clustering algorithms exist, of which we refer the reader to a specialized review discussing their advantages and disadvantages [191].

Datasets that are large in dimensionality can have adverse effects on cluster algorithms [192]. This is illustrated in a study where miRNA levels were measured from multiple cancer cell lines. When 217 miRNA targets (dimensionality of 217) were taken into account, hierarchical clustering allowed to cluster cell lines from the colon, liver, pancreas, and stomach origin together, reflecting their endodermic origin **(Figure 7C)** [193]. However, this relationship was lost when 16000 mRNA's were included in the analysis due to higher dimensionality.

Not all variables that contribute to higher dimensionality levels are relevant and thereby create noise in cluster algorithms. A method to overcome this is through principal component analysis (PCA) [194], which reduces data dimensionality. Besides a useful tool to enhance the accuracy of clustering methods, it is also frequently applied to assess visual similarities between data points. PCA simplifies dimensional complexity by geometrically projecting the data into a lower-dimensional space. This method was applied to demonstrate that a flat tissue culture surface, a flat polyimide surface, and a nanogrooved polyimide surface, induced distinct gene expression profiles independent of MSC donor variability [26]. In research where the effect of micro-topographies on chondrogenesis was assessed, PCA distinguished surfaces based on the gene expression and morphological profiles they elicit [195]. In a cytokine screening of multiple cancer cell lines cultured on different hydrogels, PCA allowed identifying biomaterials that induced similar or distinct cytokine profiles **(Figure 7D)** [196].

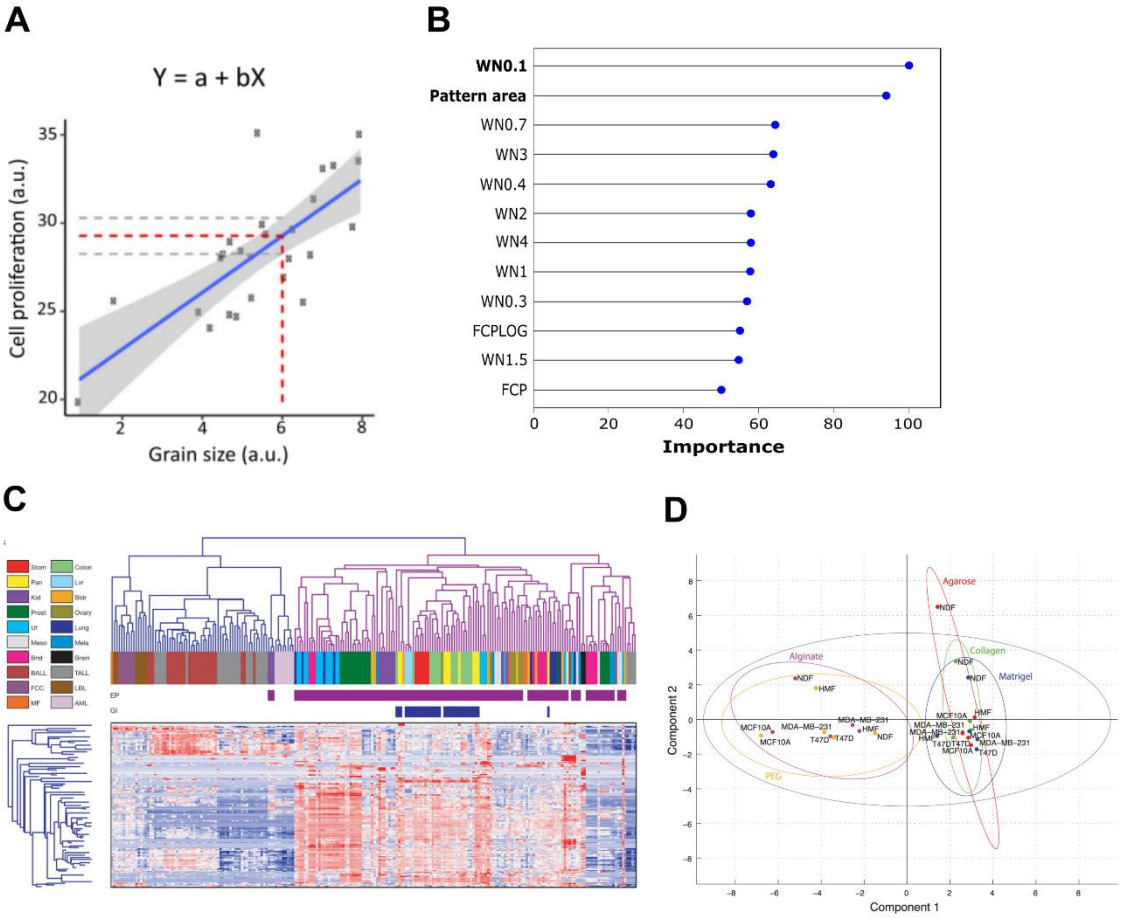

Figure 7: Machine learning examples applied in regenerative medicine research. A) Simple linear regression example. The dependent variable (Y) is predicted using the independent variable (X). Here, the output (cell proliferation) is the dependent variable, and the input (grain size) is the independent variable. Adapted with permission from [177]. Copyright (2017) Elsevier. **B)** Example of a Random Forest output. Each bar represents the importance of a surface feature characteristic associated with improved phenotypic characteristics in tenocytes. Data originates from a TopoChip screen containing 2176 different micro-topographies with Scleraxis, a tenogenic marker, as output. Adapted with permission from [51]. Copyright (2019) Elsevier. **C)** Hierarchical clustering representation of miRNA profiles from 218 tissue samples. Samples are in columns, miRNA expression in rows. Samples from the same tissue and lineage origin cluster together. Adapted with permission from [193]. Copyright (2015) Springer Nature. **D)** PCA Dimensionality reduction performed on the secretion profile from 5 different cell lines cultured on 5 different biomaterials. PCA demonstrates that in this setup, alginate and PEG induce a similar secretion profile while being distinct from agarose, collagen, and matrigel. Between cell lines, agarose induces a distinct secretion profile compared to the other cell lines cultured on the same substrate. Adapted with permission from [196]. Copyright (2017) American Chemical Society.

PCA can, in some cases, experience computational limitations, which disallows a meaningful data visualization [197]. An alternative technique that is gaining popularity for dimensionality reduction and visualization of high-dimensional datasets is t-distributed stochastic neighbor embedding (t-SNE) [198]. This method visualized different human tissues based on their respective gene expression levels [199]. Similarly, dynamic developmental processes in the zebrafish embryo were visualized through single-cell RNA sequencing of more than 92000 cells [200]. In the future, this technique will likely gain traction in high-throughput applications with highly dimensional data-sets. All the previous examples demonstrate that machine learning algorithms are useful tools for a correct data interpretation of high-throughput applications.

Discussion

Throughout this work, we presented multiple high-throughput approaches **(Table 1)**. A general disadvantage of these platforms is that the output only encompasses a few parameters, with ICC as the most prominent technique. This is attributed due to technical limitations. In the high-throughout examples we gave, there are usually insufficient cell numbers to detect meaningful RNA or protein concentrations. Nevertheless, techniques such as the aforementioned CellPaint assay can increase the screening information content [159]. Furthermore, other techniques such as mass-spectrometric imaging

Screening platform	Essential techniques	Maximal described sample size	Biological assays	References
Roughness	Etching	Gradients	ICC	[13], [18]
Surface structures	Lithography - hot embossing	2176	ICC	[26], [38], [42], [51], [52]
		Well format (96–384 samples)	ICC - Genomics/Proteomics assays	[35], [54]
Protein/polymer patterns	Microcontact printing	(1)	ICC	[60], [61], [62], [136]
	Photo patterning	(1)	ICC	[147], [148]
Polymers/hydrogels compositions	Inkjet printing	2280	ICC	[83], [86], [89], [100]
Small molecule screenings	Robotics for large sample size	100,000	ICC - Genomics/Proteomics assays	[115], [116], [117], [118], [119], [120], [121]

Table 1: Summary of different high-throughput approaches. (1) Not applied in a high-throughput context. However, depending on the layout of the lithography mask, this can be accomplished. For example, by applying the lithography mask of the TopoChip platform.

[201], and single-cell RNA sequencing, might in the future find useful high-throughput applications. When reducing the total number of input variables towards a well-plate format, other techniques such as qPCR, ELISA, RNA sequencing, and proteomics become possible due to the presence of sufficient cell numbers [35,54]. However, a strategy that is commonly employed is first to find positive hits through a high-throughput screen. Afterwards, the positive hits are fabricated in a larger format, enabling broader investigations into other markers or pathways through other techniques besides ICC [51].

Screening technologies brought new culture environments that are useful for regenerative medicine, while in parallel provided us with novel biological insights. However, the enormous complexity that exists also illustrates the challenges the field faces. Although high-throughput platforms comprise many perturbations, these are usually focused on one aspect of the cell niche. For example, different roughness levels are rarely combined with various geometric shapes, surface chemistry, and culture media compositions. Likewise, high-throughput screens that investigate multiple matrix compositions do not include surface structures or apply stretch forces. This can result in the loss of valuable information. For example, mechanical stimulation can upregulate the presence of growth factor receptors in smooth muscle cells, sensitizing them against growth factor stimulation [202]. Integrins that bind to specific matrix molecules influence growth factor activation by forming complexes with growth factor receptors [203,204]. The consequence of this can be that high-throughput screens utilizing growth factors or small molecules in a collagen substrate environment can elicit different cell behavior compared to a laminin substrate. Also, surface structures can alter cellular sensitivity against growth factors [205], and the biological activity of matrix compounds [206]. These are only a few examples of how combinatorial environments can further improve experimental outcomes and underlines the importance of employing this principle in high-throughput screens, which is still an underdeveloped concept. The main reasons for these sparse combinatorial approaches are either technical challenges or the lack of know-how.

Another interesting viewpoint is the use of databases to supplement and support data derived from high-throughput applications. Techniques such as Cell Paint that produce a morphological fingerprint [159], can further be compared with databases of other fingerprints produced by gene alterations or small molecule treatment [207,208]. In line with this are the possibilities that large scale gene expression profiling initiatives offer, such as the recent expansion of the Connectivity Map [209], which contains a million gene signatures of cell lines treated with small molecules, shRNA, and overexpression constructs. With the rise in automatization, omics technologies, and artificial intelligence, we foresee big opportunities to speed up scientific discoveries [210]. In the future, cross-high-throughput platforms involving design, chemistry, and biochemistry combined with high-content technologies will open the road to novel biological insights and regenerative medicine applications.

Acknowledgments

This project has received funding from the European Union's Horizon 2020 research and innovation programme under the Marie Skłodowska-Curie grant agreement No 676338. We gratefully thank Urnaa Tuvshindorj for sharing a figure of a RGD adhesive island based high-throughput platform.

References

1. Sharma, R. *et al.* Clinical-grade stem cell-derived retinal pigment epithelium patch rescues retinal degeneration in rodents and pigs. *Sci. Transl. Med.* **11**, 1–14 (2019).
2. Cionca, N., Müller, N. & Mombelli, A. Two-piece zirconia implants supporting all-ceramic crowns: A prospective clinical study. *Clin. Oral Implants Res.* **26**, 413–418 (2015).
3. Nicolle, L. E. Catheter associated urinary tract infections. *Antimicrob. Resist. Infect. Control* **3**, 1–8 (2014).
4. Anderson, J. M., Rodriguez, A. & Chang, D. T. Foreign body reaction to biomaterials. *Semin. Immunol.* **20**, 86–100 (2008).
5. Victor, J. *et al.* Total knee arthroplasty at 15-17 years: Does implant design affect outcome? *Int. Orthop.* **38**, 235–241 (2014).
6. Holmich, L. R. *et al.* Incidence of Silicone Breast Implant Rupture. *Arch Surg.* **138**, 801–806 (2003).
7. Groen, N. *et al.* Linking the Transcriptional Landscape of Bone Induction to Biomaterial Design Parameters. *Adv. Mater.* **29**, (2017).
8. Tare, R. S. *et al.* A microarray approach to the identification of polyurethanes for the isolation of human skeletal progenitor cells and augmentation of skeletal cell growth. *Biomaterials* **30**, 1045–1055 (2009).
9. Holtzer, H., Abbot, J., Lash, J. & S., H. The Loss of Phenotypic Traits by Differentiated Cells in vitro, I. Dedifferentiation of Cartilage Cells. *PNAS* **46**, 1533–1542 (1960).
10. Buser, D. *et al.* Influence of surface characteristics on bone integration of titanium implants. A histomorphometric study in miniature pigs. *J. Biomed. Mater. Res.* **25**, 889–902 (1991).
11. Buser, D. *et al.* Enhanced Bone Apposition to a Chemically Modified SLA Titanium Surface. *J Dent Res* **83**, 529–533 (2004).
12. Martin, J. Y. *et al.* Effect of titanium surface roughness on proliferation, differentiation, and protein synthesis of human osteoblast-like cells (MG63). *J. Biomed. Mater. Res.* **29**, 389–401 (1995).
13. Faia-Torres, A. B. *et al.* Differential regulation of osteogenic differentiation of stem cells on surface roughness gradients. *Biomaterials* **35**, 9023–9032 (2014).
14. Müller, P. *et al.* Calcium phosphate surfaces promote osteogenic differentiation of mesenchymal stem cells. *J. Cell. Mol. Med.* **12**, 281–291 (2008).
15. Jaggy, M. *et al.* Hierarchical Micro-Nano Surface Topography Promotes Long-Term Maintenance of Undifferentiated Mouse Embryonic Stem Cells. *Nano Lett.* **15**, 7146–7154 (2015).
16. Jeon, K. *et al.* Self-renewal of embryonic stem cells through culture on nanopattern polydimethylsiloxane substrate. *Biomaterials* **33**, 5206–5220 (2012).
17. Chung, T. W., Liu, D. Z., Wang, S. Y. & Wang, S. S. Enhancement of the growth of human endothelial cells by surface roughness at nanometer scale. *Biomaterials* **24**, 4655–4661 (2003).
18. Kunzler, T. P., Drobek, T., Schuler, M. & Spencer, N. D. Systematic study of osteoblast and fibroblast response to roughness by means of surface-morphology gradients. *Biomaterials* **28**, 2175–2182 (2007).
19. Werner, M. *et al.* Surface Curvature Differentially Regulates Stem Cell Migration and Differentiation via Altered Attachment Morphology and Nuclear Deformation. *Adv. Sci.* **4**, 1–11 (2017).

20. Werner, M., Kurniawan, N. A., Korus, G., Bouten, C. V. C. & Petersen, A. Mesoscale substrate curvature overrules nanoscale contact guidance to direct bone marrow stromal cell migration. *J. R. Soc. Interface* **15**, (2018).

21. Werner, M., Petersen, A., Kurniawan, N. A. & Bouten, C. V. C. Cell-Perceived Substrate Curvature Dynamically Coordinates the Direction , Speed , and Persistence of Stromal Cell Migration. *Adv. Biosyst.* **3**, (2019).

22. Baptista, D., Teixeira, L., van Blitterswijk, C., Giselbrecht, S. & Truckenmüller, R. Overlooked? Underestimated? Effects of Substrate Curvature on Cell Behavior. *Trends Biotechnol.* **37**, 838–854 (2019).

23. Zhou, Q. *et al.* Directional nanotopographic gradients: A high-throughput screening platform for cell contact guidance. *Sci. Rep.* **5**, 1–12 (2015).

24. Boon, T. A. B. Van Der, Yang, L., Li, L. & Galván, D. E. C. Well Plate Integrated Topography Gradient Screening Technology for Studying Cell-Surface Topography Interactions. *Adv. Biosyst.* **1900218**, (2019).

25. Zhou, Q. *et al.* Screening Platform for Cell Contact Guidance Based on Inorganic Biomaterial Micro/nanotopographical Gradients. *ACS Appl. Mater. Interfaces* **9**, 31433–31445 (2017).

26. Abagnale, G. *et al.* Surface topography enhances differentiation of mesenchymal stem cells towards osteogenic and adipogenic lineages. *Biomaterials* **61**, 316–326 (2015).

27. López-Bosque, M. J. *et al.* Fabrication of hierarchical micro-nanotopographies for cell attachment studies. *Nanotechnology* **24**, (2013).

28. Downing, T. L. *et al.* Biophysical regulation of epigenetic state and cell reprogramming. *Nat. Mater.* **12**, 1154–1162 (2013).

29. Abagnale, G. *et al.* Surface Topography Guides Morphology and Spatial Patterning of Induced Pluripotent Stem Cell Colonies. *Stem Cell Reports* **9**, 654–666 (2017).

30. Lee, M. R. *et al.* Direct differentiation of human embryonic stem cells into selective neurons on nanoscale ridge/groove pattern arrays. *Biomaterials* **31**, 4360–4366 (2010).

31. Mattotti, M. *et al.* Inducing functional radial glia-like progenitors from cortical astrocyte cultures using micropatterned PMMA. *Biomaterials* **33**, 1759–1770 (2012).

32. English, A. *et al.* Substrate topography: A valuable in vitro tool, but a clinical red herring for in vivo tenogenesis. *Acta Biomater.* **27**, 3–12 (2015).

33. Zhu, J. *et al.* The regulation of phenotype of cultured tenocytes by microgrooved surface structure. *Biomaterials* **31**, 6952–6958 (2010).

34. Mattotti, M. *et al.* Differential neuronal and glial behavior on flat and micro patterned chitosan films. *Colloids Surfaces B Biointerfaces* **158**, 569–577 (2017).

35. Hu, J. *et al.* High-Throughput Mechanobiology Screening Platform Using Micro- and Nanotopography. *Nano Lett.* **55**, 9557–9561 (2017).

36. Moe, A. A. K. *et al.* Microarray with micro- and nano-topographies enables identification of the optimal topography for directing the differentiation of primary murine neural progenitor cells. *Small* **8**, 3050–3061 (2012).

37. Ankam, S. *et al.* Substrate topography and size determine the fate of human embryonic stem cells to neuronal or glial lineage. *Acta Biomater.* **9**, 4535–4545 (2013).

38. Tan, K. K. B. *et al.* Enhanced differentiation of neural progenitor cells into neurons of the mesencephalic dopaminergic subtype on topographical patterns. *Biomaterials* **43**, 32–43 (2015).

39. Dalby, M. J. *et al.* The control of human mesenchymal cell differentiation using nanoscale symmetry and disorder. *Nat. Mater.* **6**, 997–1003 (2007).

40. Rasmussen, C. H. *et al.* Enhanced Differentiation of Human Embryonic Stem Cells Toward Definitive Endoderm on Ultrahigh Aspect Ratio Nanopillars. *Adv. Funct. Mater.* **26**, 815–823 (2016).

41. Kong, Y. P., Tu, C. H., Donovan, P. J. & Yee, A. F. Expression of Oct4 in human embryonic stem cells is dependent on nanotopographical configuration. *Acta Biomater.* **9**, 6369–6380 (2013).

42. Lovmand, J. *et al.* The use of combinatorial topographical libraries for the screening of enhanced osteogenic expression and mineralization. *Biomaterials* **30**, 2015–2022 (2009).

43. Kolind, K. *et al.* Control of proliferation and osteogenic differentiation of human dental-pulp-derived stem cells by distinct surface structures. *Acta Biomater.* **10**, 641–650 (2014).

44. Markert, L. D. *et al.* Identification of Distinct Topographical Surface Microstructures Favoring Either Undifferentiated Expansion or Differentiation of Murine Embryonic Stem Cells. *Stem Cells Dev.* **18**, 1331–1342 (2009).

45. Joergensen, N. L. *et al.* Topography-Guided Proliferation: Distinct Surface Microtopography Increases Proliferation of Chondrocytes *In Vitro*. *Tissue Eng. Part A* **21**, 2757–2765 (2015).

46. Kolind, K. *et al.* A combinatorial screening of human fibroblast responses on micro-structured surfaces. *Biomaterials* **31**, 9182–9191 (2010).

47. Unadkat, H. V *et al.* An algorithm-based topographical biomaterials library to instruct cell fate. *Proc. Natl. Acad. Sci. U. S. A.* **108**, 16565–70 (2011).

48. Reimer, A. *et al.* Scalable topographies to support proliferation and Oct4 expression by human induced pluripotent stem cells. *Sci. Rep.* **6**, 18948 (2016).

49. Vasilevich, A. S., Mourcin, F., Mentink, A., Hulshof, F. & Beijer, N. Designed Surface Topographies Control ICAM-1 Expression in Tonsil-Derived Human Stromal Cells. *Front. Bioeng. Biotechnol.* **6**, 1–14 (2018).

50. Hulshof, F. F. B. *et al.* Mining for osteogenic surface topographies: In silico design to in vivo osseo-integration. *Biomaterials* **137**, 49–60 (2017).

51. Vermeulen, S. *et al.* Identification of topographical architectures supporting the phenotype of rat tenocytes. *Acta Biomater.* **83**, 277–290 (2019).

52. Hulshof, F. F. B. *et al.* NanoTopoChip: High-throughput nanotopographical cell instruction. *Acta Biomater.* **62**, 188–198 (2017).

53. Beijer, N. R. M. *et al.* TopoWellPlate: A Well-Plate-Based Screening Platform to Study Cell-Surface Topography Interactions. *Adv. Biosyst.* **1**, 1700002 (2017).

54. Leuning, D. G. *et al.* The cytokine secretion profile of mesenchymal stromal cells is determined by surface structure of the microenvironment. *Sci. Rep.* **8**, 1–9 (2018).

55. Plow, E. F., Haas, T. A., Zhang, L., Loftus, J. & Smith, J. W. Ligand binding to integrins. *J. Biol. Chem.* **275**, 21785–21788 (2000).

56. Jokinen, J. *et al.* Integrin-mediated cell adhesion to type I collagen fibrils. *J. Biol. Chem.* **279**, 31956–31963 (2004).

57. Belkin, A. M. & Stepp, M. A. Integrins as receptors for laminins. *Microsc. Res. Tech.* **51**, 280–301 (2000).

58. Orlowska, A. *et al.* The effect of coatings and nerve growth factor on attachment and differentiation of Pheochromocytoma Cells. *Materials (Basel).* **11**, 1–10 (2017).

59. Hayashi, Y. *et al.* Integrins Regulate Mouse Embryonic Stem Cell Self-Renewal. *Stem Cells* **25**, 3005–3015 (2007).

60. Singhvi, R. *et al.* Engineering Cell Shape and Function. *Science (80-.).* **264**, 696–698 (1994).

61. McBeath, R., Pirone, D. M., Nelson, C. M., Bhadriraju, K. & Chen, C. S. Cell shape, cytoskeletal tension, and RhoA regulate stem cell lineage commitment. *Dev. Cell* **6**, 483–495 (2004).

62. Connelly, J. T. *et al.* Actin and serum response factor transduce physical cues from the microenvironment to regulate epidermal stem cell fate decisions. *Nat. Cell Biol.* **12**, 711–718 (2010).

63. Flaim, C. J., Chien, S. & Bhatia, S. N. An extracellular matrix microarray for probing cellular differentiation. *Nat. Methods* **2**, 119–125 (2005).

64. Kwon, S. J., Lee, M., Ku, B., Sherman, D. H. & Dordick, J. S. Defined Substrates for Human Embryonic Stem Cell Growth Identified from Surface Arrays. *ACS Chem. Biol.* **2**, 419–425 (2007).

65. Soen, Y., Mori, A., Palmer, T. D. & Brown, P. O. Exploring the regulation of human neural precursor cell differentiation using arrays of signaling microenvironments. *Mol. Syst. Biol.* **2**, 1–14 (2006).

66. Nakajima, M. *et al.* Combinatorial protein display for the cell-based screening of biomaterials that direct neural stem cell differentiation. *Biomaterials* **28**, 1048–1060 (2007).

67. Neto, A. I., Custódio, C. A., Song, W. & Mano, J. F. High-throughput evaluation of interactions between biomaterials, proteins and cells using patterned superhydrophobic substrates. *Soft Matter* **7**, 4147–4151 (2011).

68. Tzoneva, R., Faucheux, N. & Groth, T. Wettability of substrata controls cell-substrate and cell-cell adhesions. *Biochim. Biophys. Acta - Gen. Subj.* **1770**, 1538–1547 (2007).

69. Van Kooten, T. G., Spijker, H. T. & Busscher, H. J. Plasma-treated polystyrene surfaces: Model surfaces for studying cell-biomaterial interactions. *Biomaterials* **25**, 1735–1747 (2004).

70. Mitchell, S. A. *et al.* Cellular attachment and spatial control of cells using micro-patterned ultra-violet/Ozone treatment in serum enriched media. *Biomaterials* **25**, 4079–4086 (2004).

71. Mitchell, S. A., Poulsson, A. H. C., Davidson, M. R. & Bradley, R. H. Orientation and confinement of cells on chemically patterned polystyrene surfaces. *Colloids Surfaces B Biointerfaces* **46**, 108–116 (2005).

72. Poulsson, A. H. C., Mitchell, S. A., Davidson, M. R., Emmison, N. & Bradley, R. H. Adhesion of primary human osteoblast cells to UV/ozone modified polyethylene. *Langmuir* **25**, 3718–3727 (2009).

73. Grinnell, F. & Feld, M. K. Fibronectin adsorption on hydrophilic and hydrophobic surfaces detected by antibody binding and analyzed during cell adhesion in serum-containing medium. *J. Biol. Chem.* **257**, 4888–4893 (1982).

74. Keselowsky, B. G., Collard, D. M. & García, A. J. Surface chemistry modulates fibronectin conformation and directs integrin binding and specificity to control cell adhesion. *J. Biomed. Mater. Res. Part A* **66A**, 247–259 (2003).

75. Urquhart, A. J. *et al.* High throughput surface characterisation of a combinatorial material library. *Adv. Mater.* **19**, 2486–2491 (2007).

76. Thaburet, J. F., Mizomoto, H. & Bradley, M. High-Throughput Evaluation of the Wettability of Polymer Libraries. *Macromol. Rapid Commun.* **25**, 366–370 (2004).

77. Weber, N., Bolikal, D., Bourke, S. L. & Kohn, J. Small changes in the polymer structure influence the adsorption behavior of fibrinogen on polymer surfaces: Validation of a new rapid screening technique. *J. Biomed. Mater. Res. - Part A* **68**, 496–503 (2004).

78. Maitz, M. F. Applications of synthetic polymers in clinical medicine. *Biosurface and Biotribology* **1**, 161–176 (2015).

79. Tourniaire, G. *et al.* Polymer microarrays for cellular adhesion. *Chem. Commun.* 2118–2120 (2006). doi:10.1039/b602009g

80. Anderson, D. G., Putnam, D., Lavik, E. B., Mahmood, T. A. & Langer, R. Biomaterial microarrays: Rapid, microscale screening of polymer-cell interaction. *Biomaterials* **26**, 4892–4897 (2005).

81. Pernagallo, S., Diaz-Mochon, J. J. & Bradley, M. A cooperative polymer-DNA microarray approach to biomaterial investigation. *Lab Chip* **9**, 397–403 (2009).

82. Treiser, M. D. *et al.* Cytoskeleton-based forecasting of stem cell lineage fates. *Proc. Natl. Acad. Sci. U. S. A.* **107**, 610–615 (2010).

83. Anderson, D. G., Levenberg, S. & Langer, R. Nanoliter-scale synthesis of arrayed biomaterials and application to human embryonic stem cells. *Nat. Biotechnol.* **22**, 863–866 (2004).

84. Meredith, J. C. *et al.* Combinatorial characterization of cell interactions with polymer surfaces. *J. Biomed. Mater. Res., Part A* **66A**, 483–490 (2003).

85. Rasi Ghaemi, S. *et al.* High-Throughput Assessment and Modeling of a Polymer Library Regulating Human Dental Pulp-Derived Stem Cell Behavior. *ACS Appl. Mater. Interfaces* **10**, 38739–38748 (2018).

86. Hay, D. C. *et al.* Unbiased screening of polymer libraries to define novel substrates for functional hepatocytes with inducible drug metabolism. *Stem Cell Res.* **6**, 92–102 (2011).

87. Mei, Y. *et al.* Combinatorial development of biomaterials for clonal growth of human pluripotent stem cells. *Nat. Mater.* **9**, 768–778 (2010).

88. Yang, J. *et al.* Polymer surface functionalities that control human embryoid body cell adhesion revealed by high throughput surface characterization of combinatorial material microarrays. *Biomaterials* **31**, 8827–8838 (2010).

89. Hook, A. L. *et al.* Combinatorial discovery of polymers resistant to bacterial attachment. *Nat. Biotechnol.* **30**, 868–875 (2012).

90. Sanni, O. *et al.* Bacterial attachment to polymeric materials correlates with molecular flexibility and hydrophilicity. *Adv. Healthc. Mater.* **4**, 695–701 (2015).

91. Hook, A. L. *et al.* Discovery of novel materials with broad resistance to bacterial attachment using combinatorial polymer microarrays. *Adv. Mater.* **25**, 2542–2547 (2013).

92. Brocchini, S., James, K., Tangpasuthadol, V. & Kohn, J. Structure-property correlations in a combinatorial library of degradable biomaterials. *J. Biomed. Mater. Res.* **42**, 66–75 (1998).

93. Engler, A. J., Sen, S., Sweeney, H. L. & Discher, D. E. Matrix Elasticity Directs Stem Cell Lineage Specification. *Cell* **126**, 677–689 (2006).

94. Gilbert, P. *et al.* Substrate elasticity regulates skeletal muscle stem cell self-renewal in culture. *Science (80-.).* **329**, 1078–1081 (2011).

95. Gobaa, S. *et al.* Artificial niche microarrays for probing single stem cell fate in high throughput. *Nat. Methods* **8**, 949–955 (2011).

96. Ranga, A. *et al.* 3D niche microarrays for systems-level analyses of cell fate. *Nat. Commun.* **5**, 1–10 (2014).

97. Usprech, J., Romero, D. A., Amon, C. H. & Simmons, C. A. Combinatorial screening of 3D biomaterial properties that promote myofibrogenesis for mesenchymal stromal cell-based heart valve tissue engineering. *Acta Biomater.* **58**, 34–43 (2017).

98. Liu, H. *et al.* Microdevice arrays with strain sensors for 3D mechanical stimulation and monitoring of engineered tissues. *Biomaterials* **172**, 30–40 (2018).

99. Duffy, C., Venturato, A., Callanan, A., Lilienkampf, A. & Bradley, M. Arrays of 3D double-network hydrogels for the high-throughput discovery of materials with enhanced physical and biological properties. *Acta Biomater.* **34**, 104–112 (2016).

100. Zhang, R., Liberski, A., Sanchez-Martin, R. & Bradley, M. Microarrays of over 2000 hydrogels - Identification of substrates for cellular trapping and thermally triggered release. *Biomaterials* **30**, 6193–6201 (2009).

101. Kumachev, A. *et al.* High-throughput generation of hydrogel microbeads with varying elasticity for cell encapsulation. *Biomaterials* **32**, 1477–1483 (2011).

102. Iansante, V., Dhawan, A., Masmoudi, F. & Lee, C. A. A New High Throughput Screening Platform for Cell Encapsulation in Alginate Hydrogel Shows Improved Hepatocyte Functions by Mesenchymal Stromal Cells. *Front. Med.* **5**, 1–11 (2018).

103. Li Jeon, N. *et al.* Neutrophil chemotaxis in linear and complex gradients of interleukin-8 formed in a microfabricated device. *Nat. Biotechnol.* **20**, 826–830 (2002).

104. Chiu, D. T. *et al.* Patterned deposition of cells and proteins onto surfaces by using three-dimensional microfluidic systems. *Proc. Natl. Acad. Sci.* **97**, 2408–2413 (2000).

105. Barata, D., Provaggi, E., Van Blitterswijk, C. & Habibovic, P. Development of a microfluidic platform integrating high-resolution microstructured biomaterials to study cell-material interactions. *Lab Chip* **17**, 4134–4147 (2017).

106. Huh, D. *et al.* A human disease model of drug toxicity-induced pulmonary edema in a lung-on-a-chip microdevice. *Sci. Transl. Med.* **4**, (2012).

107. Barata, D., Van Blitterswijk, C. & Habibovic, P. High-throughput screening approaches and combinatorial development of biomaterials using microfluidics. *Acta Biomater.* **34**, 1–20 (2016).

108. Mi, S. *et al.* Microfluidic co-culture system for cancer migratory analysis and anti-metastatic drugs screening. *Sci. Rep.* **6**, 1–11 (2016).

109. Zhang, Y., Zhang, W. & Qin, L. Mesenchymal-Mode Migration Assay and Antimetastatic Drug Screening via High Throughput Microfluidics Channel Networks. *Angew Chem Int Ed Engl* **38**, 469–485 (2014).

110. Chung, B. G. *et al.* Human neural stem cell growth and differentiation in a gradient-generating microfluidic device. *Lab Chip* **5**, 401–406 (2005).

111. Kim, J. H., Sim, J. & Kim, H. J. Neural stem cell differentiation using microfluidic device-generated growth factor gradient. *Biomol. Ther.* **26**, 380–388 (2018).

112. Occhetta, P., Visone, R. & Rasponi, M. High-throughput microfluidic platform for 3D cultures of mesenchymal stem cells. *Sci. Rep.* **1612**, 303–323 (2017).

113. Klein, A. M., Mazutis, L., Akartuna, I., Tallapragada, N. & Veres, A. Droplet barcoding for single cell transcriptomics applied to embryonic stem cells. *Cell* **161**, 1187–1201 (2016).

114. Caen, O., Lu, H., Nizard, P. & Taly, V. Microfluidics as a Strategic Player to Decipher Single-Cell Omics? *Trends Biotechnol.* **35**, 713–727 (2017).

115. Ben-David, U. *et al.* Selective elimination of human pluripotent stem cells by an oleate synthesis inhibitor discovered in a high-throughput screen. *Cell Stem Cell* **12**, 167–179 (2013).

116. Borowiak, M. *et al.* Small Molecules Efficiently Direct Endodermal Differentiation of Mouse and Human Embryonic Stem Cells. *Cell Stem Cell* **4**, 348–358 (2009).

117. Ding, S. *et al.* Synthetic small molecules that control stem cell fate. *PNAS* **100**, 7632–7637 (2003).

118. Alves, H., Dechering, K., van Blitterswijk, C. & de Boer, J. High-throughput assay for the identification of compounds regulating osteogenic differentiation of human mesenchymal stromal cells. *PLoS One* **6**, 2–11 (2011).

119. Chen, S. *et al.* Self-renewal of embryonic stem cells by a small molecule. *Proc. Natl. Acad. Sci.* **103**, 17266–17271 (2006).

120. Le, B. q. *et al.* High-Throughput Screening Assay for the Identification of Compounds Enhancing Collagenous Extracellular Matrix Production by ATDC5 Cells. *Tissue Eng. Part C Methods* **21**, 726–736 (2015).

121. Doorn, J. *et al.* A small molecule approach to engineering vascularized tissue. *Biomaterials* **34**, 3053–3063 (2013).

122. Westbroek, P. & Marin, F. A marriage of bone and nacre. *Nature* **392**, 861–862 (1998).

123. Crubzy, E., Murail, P., Girard, L. & Bernadou, J.-P. False teeth of the Roman world. *Nature* **391**, 29–29 (1998).

124. Nerlich, A. G., Zink, A., Szeimies, U. & Hagedorn, H. G. Ancient Egyptian prosthesis of the big toe. *Lancet* **356**, 2176–2179 (2000).

125. Zhao, Y. *et al.* High-definition micropatterning method for hard, stiff and brittle polymers. *Mater. Sci. Eng. C* **71**, 558–564 (2017).

126. Kurpinski, K., Chu, J., Hashi, C. & Li, S. Anisotropic mechanosensing by mesenchymal stem cells. *Proc. Natl. Acad. Sci. U. S. A.* **103**, 16095–100 (2006).

127. Berthier, E., Young, E. W. K. & Beebe, D. Engineers are from PDMS-land, biologists are from polystyrenia. *Lab Chip*

12, 1224–1237 (2012).

128. Goral, V. N., Hsieh, Y. C., Petzold, O. N., Faris, R. A. & Yuen, P. K. Hot embossing of plastic microfluidic devices using poly(dimethylsiloxane) molds. *J. Micromechanics Microengineering* **21**, (2011).

129. Peng, L., Deng, Y., Yi, P. & Lai, X. Micro hot embossing of thermoplastic polymers: A review. *J. Micromechanics Microengineering* **24**, (2014).

130. Santini, A., Gallegos, I. T. & Felix, C. M. Photoinitiators in dentistry: a review. *Prim. Dent. J.* **2**, 30–33 (2013).

131. Çiçek, Ç., Çakmakçi, E., Kayaman-Apohan, N., Arslan, M. & Erdem Kuruca, S. Fabrication of PLGA based tissue engineering scaffolds via photocuring and salt leaching techniques. *Int. J. Polym. Mater. Polym. Biomater.* **62**, 719–725 (2013).

132. Choi, J. R., Yong, K. W., Choi, J. Y. & Cowie, A. C. Recent Advances in Hydrogels for Biomedical Applications. *Biotechniques* **66**, 40–53 (2019).

133. Vrij, E. J. *et al.* 3D high throughput screening and profiling of embryoid bodies in thermoformed microwell plates. *Lab Chip* **16**, 734–742 (2016).

134. Mair, D. A., Geiger, E., Pisano, A. P., Fréchet, J. M. J. & Svec, F. Injection molded microfluidic chips featuring integrated interconnects. *Lab Chip* **6**, 1346–1354 (2006).

135. Truckenmüller, R. *et al.* Thermoforming of film-based biomedical microdevices. *Adv. Mater.* **23**, 1311–1329 (2011).

136. Tu, C. *et al.* A Microfluidic Chip for Cell Patterning Utilizing Paired Microwells and Protein Patterns. *Micromachines* **8**, (2017).

137. Kane, R. S., Takayama, S., Ostuni, E., Ingber, D. E. & Whitesides, G. M. Patterning proteins and cells using soft lithography. *Biomaterials* **20**, 2363–2376 (1999).

138. Duan, X. *et al.* High-resolution contact printing with chemically patterned flat stamps fabricated by nanoimprint lithography. *Adv. Mater.* **21**, 2798–2802 (2009).

139. Granlund, T., Nyberg, T., Stolz Roman, L., Svensson, M. & Inganäs, O. Patterning of polymer light-emitting diodes with soft lithography. *Adv. Mater.* **12**, 269–273 (2000).

140. Bennett, R. D. *et al.* Creating patterned carbon nanotube catalysts through the microcontact printing of block copolymer micellar thin films. *Langmuir* **22**, 8273–8276 (2006).

141. Wang, M., Braun, H. G. & Meyer, E. Patterning of polymeric/inorganic nanocomposite and nanoparticle layers. *Chem. Mater.* **14**, 4812–4818 (2002).

142. Alom, S. & Chen, C. S. Microcontact printing : A tool to pattern. *Soft Matter* **3**, 168–177 (2006).

143. Nie, Z. & Kumacheva, E. Patterning surfaces with functional polymers. *Nat. Mater.* **7**, 277–290 (2008).

144. Kaufmann, T. & Ravoo, B. J. Stamps, inks and substrates: Polymers in microcontact printing. *Polym. Chem.* **1**, 371–387 (2010).

145. Zhang, R., Liberski, A., Khan, F., Diaz-Mochon, J. J. & Bradley, M. Inkjet fabrication of hydrogel microarrays using in situ nanolitre-scale polymerisation. *Chem. Commun.* 1317–1319 (2008). doi:10.1039/b717932d

146. De Gans, B. J., Duineveld, P. C. & Schubert, U. S. Inkjet printing of polymers: State of the art and future developments. *Adv. Mater.* **16**, 203–213 (2004).

147. Balakirev, M. Y. *et al.* Photochemical patterning of biological molecules inside a glass capillary. *Anal. Chem.* **77**, 5474–5479 (2005).

148. Kim, M. *et al.* Addressable micropatterning of multiple proteins and cells by microscope projection photolithography based on a protein friendly photoresist. *Langmuir* **26**, 12112–12118 (2010).

149. R Core Team. R: A language and environment for statistical computing. *R Found. Stat. Comput.*

150. Reference, P. L. Python Software Foundation.

151. RStudio Team. RStudio: Integrated Development for R. (2015).

152. Carpenter, A. E. *et al.* CellProfiler: image analysis software for identifying and quantifying cell phenotypes. *Genome Biol.* **7**, R100 (2006).

153. Schindelin, J. *et al.* Fiji - an Open platform for biological image analysis. *Nat. Methods* **9**, 241 (2009).

154. Mierswa, I. & Klinkenberg, R. RapidMiner Studio. (2018).

155. Ramakrishnaiah Siddappa, Ruud Licht, Clemens van Blitterswijk, J. de B. Donor Variation and Loss of Multipotency during In Vitro Expansion of Human Mesenchymal Stem Cells for Bone Tissue Engineering. *J. Orthop. Res.* (2007). doi:10.1002/jor.20402

156. Leek, J. T. *et al.* Tackling the widespread and critical impact of batch effects in high-throughput data. *Nat. Rev. Genet.* **11**, 733–739 (2010).

157. Leek, J. T. & Storey, J. D. Capturing heterogeneity in gene expression studies by surrogate variable analysis. *PLoS Genet.* **3**, 1724–1735 (2007).

158. Zijl, S. *et al.* Micro-scaled topographies direct differentiation of human epidermal stem cells. *Acta Biomater.* (2018). doi:10.1016/j.actbio.2018.12.003

159. Bray, M.-A. *et al.* Cell Painting, a high-content image-based assay for morphological profiling using multiplexed fluorescent dyes. *Nat. Protoc.* **11**, 049817 (2016).

160. McQuin, C. *et al.* CellProfiler 3.0: Next-generation image processing for biology. *PLoS Biol.* **16**, 1–17 (2018).

161. Moffat, J. *et al.* A Lentiviral RNAi Library for Human and Mouse Genes Applied to an Arrayed Viral High-Content Screen. *Cell* **124**, 1283–1298 (2006).

162. Wen, J. H. *et al.* Interplay of matrix stiffness and protein tethering in stem cell differentiation. *Nat. Mater.* **13**, 979–987 (2014).

163. Diem, K. *et al.* Image analysis for accurately counting CD4+ and CD8+ T cells in human tissue. *J. Virol. Methods* **222**, 117–121 (2015).

164. Tollemar, V. *et al.* Quantitative chromogenic immunohistochemical image analysis in cellprofiler software. *Cytom. Part A* 1–9 (2018). doi:10.1002/cyto.a.23575

165. Caicedo, J. C. *et al.* Nucleus segmentation across imaging experiments: the 2018 Data Science Bowl. *Nat. Methods* **16**, 1247–1253 (2019).

166. Caicedo, J. C. *et al.* Evaluation of Deep Learning Strategies for Nucleus Segmentation in Fluorescence Images. *Cytom. Part A* **95**, 952–965 (2019).

167. Sommer, C., Hoefler, R., Samwer, M. & Gerlich, D. W. A deep learning and novelty detection framework for rapid phenotyping in high-content screening. *Mol. Biol. Cell* **28**, 3428–3436 (2017).

168. Doan, M. *et al.* Label-Free Leukemia Monitoring by Computer Vision. *Cytom. Part A* (2020). doi:10.1002/cyto.a.23987

169. Jeyaraj, P. R. & Samuel Nadar, E. R. Computer-assisted medical image classification for early diagnosis of oral cancer employing deep learning algorithm. *J. Cancer Res. Clin. Oncol.* **145**, 829–837 (2019).

170. Urban, G. *et al.* Deep Learning Localizes and Identifies Polyps in Real Time With 96% Accuracy in Screening Colonoscopy. *Gastroenterology* **155**, 1069-1078.e8 (2018).

171. Ronneberger, O., Fisher, P. & Brox, T. U-Net: Convolutional Networks for Biomedical Image Segmentation. *MICCAI* **9351**, 234–241 (2015).

172. Sadanandan, S. K., Ranefall, P., Guyader, S. Le & Wählby, C. Automated Training of Deep Convolutional Neural Networks for Cell Segmentation. *Sci. Rep.* **7**, 1–7 (2017).

173. Yang, S. J. *et al.* Assessing microscope image focus quality with deep learning. *BMC Bioinformatics* **19**, 1–9 (2018).

174. Van Valen, D. A. *et al.* Deep Learning Automates the Quantitative Analysis of Individual Cells in Live-Cell Imaging Experiments. *PLoS Comput. Biol.* **12**, 1–24 (2016).

175. Moen, E. *et al.* Deep learning for cellular image analysis. *Nat. Methods* **16**, 1233–1246 (2019).

176. Fourcade, A. & Khonsari, R. H. Deep learning in medical image analysis: A third eye for doctors. *J. Stomatol. Oral Maxillofac. Surg.* **120**, 279–288 (2019).

177. Vasilevich, A. S., Carlier, A., de Boer, J. & Singh, S. How Not To Drown in Data: A Guide for Biomaterial Engineers. *Trends Biotechnol.* **35**, 743–755 (2017).

178. Irrechukwu, O. N. *et al.* Characterization of Engineered Cartilage Constructs Using Multiexponential T_2 Relaxation Analysis and Support Vector Regression. *Tissue Eng. Part C Methods* **18**, 433–443 (2012).

179. Bakker, D. P. *et al.* Multiple linear regression analysis of bacterial deposition to polyurethane coatings after conditioning film formation in the marine environment. *Microbiology* **150**, 1779–1784 (2004).

180. Sun, Y., Liu, Y., Wang, G. & Zhang, H. Deep Learning for Plant Identification in Natural Environment. *Comput. Intell. Neurosci.* **2017**, (2017).

181. Fukunaga, K. & Narendra, P. M. A Branch and Bound Algorithm for Computing k-Nearest Neighbors. *IEEE Trans. Comput.* **C**–**24**, 750–753 (1975).

182. Breiman, L. Random forests. *Mach. Learn.* **45**, 5–32 (2001).

183. Steinwart, I. & Christmann, A. *Support Vector Machines*. (Springer, 2008).

184. Lecun, Y., Bengio, Y. & Hinton, G. Deep learning. *Nature* **521**, 436–444 (2015).

185. Epa, V. C., Yang, J., Mei, Y., Hook, A. L. & Langer, R. Modelling human embryoid body cell adhesion to a combinatorial library of polymer surfaces. *J Mater Chem* **22**, 20902–20906 (2012).

186. MacQueen, J. Some Methods for Classification and Analysis of Multivaraite Observations. *Proc. Fifth Berkeley Symp. Math. Stat. Prob.* **1**, 281–297 (1967).

187. Stuart, R. O., Bush, K. T. & Nigam, S. K. Changes in global gene expression patterns during development and maturation of the rat kidney . *Proc. Natl. Acad. Sci. U. S. A.* **98**, 5649–5654 (2001).

188. Tanaka, T. S. *et al.* Gene Expression Profiling of Embryo-Derived Stem Cells Reveals Candidate Genes Associated With Pluripotency and Lineage Specificity. *Genome Res.* **12**, 1921–1928 (2014).

189. Winkler, R., Klawonn, F. & Kruse, R. Fuzzy C-means in high dimensional spaces. *Int. J. Fuzzy Syst. Appl.* **1**, 1–16 (2011).

190. Kumar, G. *et al.* The determination of stem cell fate by 3D scaffold structures through the control of cell shape. *Biomaterials* **32**, 9188–9196 (2011).

191. Xu, R. & Wunsch, D. C. Clustering algorithms in biomedical research: A review. *IEEE Rev. Biomed. Eng.* **3**, 120–154 (2010).

192. Ronan, T., Qi, Z. & Naegle, K. M. Avoiding common pitfalls when clustering biological data. *Sci. Signal.* **9**, (2016).

193. Lu, J. *et al.* MicroRNA expression profiles classify human cancers. *Nature* **435**, 834–838 (2005).

194. Wold, S., Esbensen, K. I. M. & Geladi, P. Principal Component Analysis. *Chemom. Intell. Lab. Syst.* **2**, 37–52 (1987).

195. Bach. Le, A. Vasilevich, S. Vermeulen, F. Hulshof, F. Stamatialis, C. van Blitterswijk, J. de B. Micro-Topographies Promote Late Chondrogenic Differentiation Markers in the ATDC5 Cell Line. *Tissue Eng. Part A* **23**, 458–469 (2017).

196. Regier, M. C. *et al.* The Influence of Biomaterials on Cytokine Production in 3D Cultures. *Biomacromolecules* **18**, 709–718 (2017).

197. Lever, J., Krzywinski, M. & Altman, N. Principal component analysis. *Nat. Methods* **14**, 641–642 (2017).

198. van der Maaten, L. & Hinton, G. Visualizing Data using t-SNE. *J. Mach. Learn. Res.* **9**, 2579–2605 (2018).

199. Taskesen, E. & Reinders, M. J. T. 2D representation of transcriptomes by t-SNE exposes relatedness between human tissues. *PLoS One* **11**, 1–6 (2016).

200. Wagner, D. E. *et al.* Single-cell mapping of gene expression landscapes and lineage in the zebrafish embryo. *Science (80-.).* **360**, 981–987 (2018).

201. Luxembourg, S. L., Mize, T. H., McDonnell, L. A. & Heeren, R. M. A. High-spatial resolution mass spectrometric imaging of peptide and protein distributions on a surface. *Anal. Chem.* **76**, 5339–5344 (2004).

202. Iwasaki, H., Eguchi, S., Ueno, H., Marumo, F. & Hirata, Y. Mechanical stretch stimulates growth of vascular smooth muscle cells via epidermal growth factor receptor. *Am. J. Physiol. Heart Circ. Physiol.* **278**, H521-9 (2000).

203. Ashe, H. L. Modulation of BMP signalling by integrins. *Biochem. Soc. Trans.* **44**, 1465–1473 (2016).

204. Worthington, J. J., Klementowicz, J. E. & Travis, M. A. TGFβ: A sleeping giant awoken by integrins. *Trends Biochem. Sci.* **36**, 47–54 (2011).

205. Wang, W. *et al.* Induction of predominant tenogenic phenotype in human dermal fibroblasts via synergistic effect of TGF-beta and elongated cell shape. *Am. J. Physiol. Cell Physiol.* ajpcell.00300.2015 (2015). doi:10.1152/ajpcell.00300.2015

206. Mateos-Timoneda, M. A., Castano, O., Planell, J. A. & Engel, E. Effect of structure, topography and chemistry on fibroblast adhesion and morphology. *J. Mater. Sci. Mater. Med.* **25**, 1781–1787 (2014).

207. Rohban, M. H. *et al.* Systematic morphological profiling of human gene and allele function via cell painting. *Elife* **6**, 1–23 (2017).

208. Bray, M. *et al.* A dataset of images and morphological profiles of 30 000 small-molecule treatments using the Cell Painting assay. *Giga Sci.* **6**, 1–5 (2017).

209. Subramanian, A. *et al.* A Next Generation Connectivity Map: L1000 Platform and the First 1,000,000 Profiles. *Cell* **171**, 1437-1452.e17 (2017).

210. Vasilevich, A. & de Boer, J. Robot-scientists will lead tomorrow's biomaterials discovery. *Curr. Opin. Biomed. Eng.* **6**, 74–80 (2018).

211. Pan, F. *et al.* Topographic effect on human induced pluripotent stem cells differentiation towards neuronal lineage. *Biomaterials* **34**, 8131–8139 (2013).